

Carbon budget estimation of a subarctic catchment using a dynamic ecosystem model at high spatial resolution

Jing Tang^{1,2}, Paul A. Miller¹, Andreas Persson¹, David Olefeldt³, Petter Pilesjö¹, Michal Heliasz¹, Marcin Jackowicz-Korczynski¹, Zhenlin Yang⁴, Benjamin Smith¹, Terry V. Callaghan^{5,6,7}, Torben R. Christensen^{1,8}

[1]{Department of Physical Geography and Ecosystem Science, Lund University, Sölvegatan 12, SE-223 62, Lund, Sweden}

[2]{Department of Resource and Environmental Science, Wuhan University, Road Luoyu 129, Wuhan, China}

[3]{Department of Renewable Resources, University of Alberta, Edmonton, AB T6G 2H1, Canada}

[4]{Department of Forest Ecosystems and Society, Oregon State University, Corvallis, 973 31, Oregon, USA}

[5]{Royal Swedish Academy of Sciences, Lilla Frescativägen 4A, 114 18, Stockholm, Sweden}

[6]{Department of Animal and Plant Sciences, University of Sheffield, S10 2TN Sheffield, UK}

[7]{Department of Botany, National Research Tomsk State University, 36, Lenin Ave., Tomsk, 634050, Russia}

[8]{Arctic Research Centre, Aarhus University, C.F. Møllers Allé 8, 8000 Aarhus C, Denmark}

Abstract

A large amount of organic carbon is stored in high latitude soils. A substantial proportion of this carbon stock is vulnerable and may decompose rapidly due to temperature increases that are

1 already greater than the global average. It is therefore crucial to quantify and understand carbon
2 exchange between the atmosphere and subarctic/arctic ecosystems. In this paper, we combine an
3 Arctic-enabled version of the process-based dynamic ecosystem model, LPJ-GUESS (version
4 LPJG-WHyMe-TFM) with comprehensive observations of terrestrial and aquatic carbon fluxes
5 to simulate long-term carbon exchange in a subarctic catchment at 50 m resolution. Integrating
6 the observed carbon fluxes from aquatic systems with the modelled terrestrial carbon fluxes
7 across the whole catchment, we estimate that the area is a carbon sink at present, and will
8 become an even stronger carbon sink by 2080, which is mainly a result of a projected
9 densification of birch forest and its encroachment into tundra heath. However, the magnitudes of
10 the modelled sinks are very dependent on future atmospheric CO₂ concentrations. Furthermore,
11 comparisons of global warming potentials between two simulations with and without CO₂
12 increase since 1960 reveal that the increased methane emission from the peatland could double
13 the warming effects of the whole catchment by 2080 in the absence of CO₂ fertilization of the
14 vegetation. This is the first process-based model study of the temporal evolution of a catchment-
15 level carbon budget at high spatial resolution, including both terrestrial and aquatic carbon.
16 Though this study also highlights some limitations in modelling subarctic ecosystem responses to
17 climate change, such as, aquatic system flux dynamics, nutrient limitation, herbivory and other
18 disturbances and peatland expansion, our study provides one process-based approach to
19 resolving the complexity of carbon cycling in subarctic ecosystems while simultaneously
20 pointing out the key model developments for capturing complex subarctic processes.

21

22 **1 Introduction**

23 The high latitudes are experiencing greater temperature increases than the global average
24 (AMAP, 2012; IPCC, 2013). Low decomposition rates due to the cold environment have led to
25 an accumulation of large carbon (C) pools in litter, soils and peatlands, much of which is
26 currently held in permafrost (Tarnocai et al., 2009; Koven et al., 2011; Hartley et al., 2012).
27 However, these C stores may be mineralized rapidly to the atmosphere due to the warming
28 effects on soil microbial activity and thereby increase atmospheric concentrations of both carbon
29 dioxide (CO₂) and methane (CH₄). Meanwhile, temperature-induced vegetation changes may

1 mitigate those effects by photosynthetic enhancement, which is, however, greatly influenced by
2 disturbances such as plant-herbivore interactions as well as soil water and nutrient contents
3 (Jonasson and Michelsen, 1996; Van Bogaert et al., 2009; Keuper et al., 2012). It is becoming
4 crucial to understand those aspects of vulnerable high latitude ecosystems and their responses to
5 climate warming (Callaghan et al., 2013). Ecosystems fix atmospheric C through photosynthesis
6 and return this C back through diverse paths and in different forms. In recent years, many field
7 measurements have been carried out in subarctic and arctic environments to quantify C
8 exchanges between the atmosphere and the biosphere. Those measurements enable us to better
9 understand possible feedbacks from terrestrial biota and responses to the changing climate
10 (Bäckstrand et al., 2010; Christensen et al., 2012). However, some concerns about field
11 measurements in the subarctic/arctic environment have been raised and the following research
12 needs have been identified:

13 1) Complete year-around observations are generally missing and many studies focus
14 only on growing season measurements (Grogan and Jonasson, 2006; Roulet et al., 2007;
15 Christensen et al., 2012; McGuire et al., 2012). Year-around observations are needed because
16 there is clear evidence that C fluxes in the cold seasons are very important (Larsen et al., 2007b;
17 Mastepanov et al., 2008).

18 2) Observations of interactions between terrestrial and aquatic systems are lacking
19 (Lundin et al., 2013; Olefeldt et al., 2013). Quantifications of terrestrial lateral loss of C are
20 needed not only because they represent a significant fraction of net ecosystem exchange (NEE)
21 but also because they are intrinsically linked to downstream aquatic C cycling (Lundin et al.,
22 2013). Integrating terrestrial and aquatic C cycling is of high importance for our understanding
23 of the C balance at the catchment scale, particularly at high latitudes. Northern peatlands are
24 large sources of dissolved organic carbon (DOC), while receiving lakes generally are net sources
25 of both CO₂ and CH₄ (Tranvik et al., 2009).

26 Many environmental characteristics of the Stordalen catchment, located in the subarctic
27 discontinuous permafrost region of northern Sweden, have been measured since the 1950s
28 (Bäckstrand, 2008) and many studies covering a variety of disciplines are still on-going
29 (Callaghan et al., 2010; Callaghan et al., 2013). Observations related to the dynamics of almost

1 all the relevant C components have been made in different landcover types (Christensen et al.,
2 2012; Callaghan et al., 2013). However, the various observations over different landcover types
3 have not yet been integrated into a comprehensive, year-round catchment-level C budget. A
4 significant aspect of this area is that it contains permafrost that is rapidly thawing (Åkerman and
5 Johansson, 2008). This makes more C hydrologically available (Olefeldt and Roulet, 2012) and
6 the large stock of C in these tundra soils becomes available to microbial processes (Sjögersten
7 and Wookey, 2002; Fox et al., 2008; Hartley et al., 2012). A rapid changing environment
8 together with comprehensive observations have established the unique importance of this area as
9 a model system for furthering our process-based understanding of the role of climate changes in
10 northern regions. Furthermore, this understanding, gained in an accessible and highly
11 instrumented area, can be applied to vast areas where large C stocks exist but long term
12 measurements are lacking.

13 The Stordalen catchment contains several distinct landcover types, including tundra heath, birch
14 forest with heath understory, peatlands and lakes/rivers. Hereafter, the peatland is divided into
15 three groups named “palsa”, “*Sphagnum* site” and “*Eriophorum* site”, based on surface
16 hydrology, permafrost condition as well as characteristic plant communities. An earlier
17 compilation of the C balance of the larger Torneträsk catchment, which encompasses the
18 Stordalen catchment, indicated that there was a significant sink capacity in the birch forest as
19 well as across the peatland (Christensen et al., 2007). This assessment, however, lacked year-
20 around measurement of CO₂ and CH₄ emissions and did not include direct measurements of
21 aquatic C fluxes (Christensen et al., 2007). Subsequent observations in the Stordalen catchment
22 have focused on filling the missing components. Consequently, recently updated year-around
23 CO₂ and CH₄ measurements in the peatland identified the wetter non-permafrost *Eriophorum*
24 sites to be strong C sinks (-46 gC/m²/yr) with high CH₄ emissions (18-22 gC/m²/yr) (Jackowicz-
25 Korczyński et al., 2010; Christensen et al., 2012), while measurements conducted on the drier
26 palsa (where permafrost is present) showed a relatively weaker uptake (-39.44 gC/m²/yr)
27 (Olefeldt et al., 2012). Total waterborne C exports (DOC plus particulate organic C (POC) and
28 dissolved inorganic C (DIC)) from the terrestrial ecosystems (both peatland and forest) were also
29 monitored (Olefeldt et al., 2013) and found to represent a significant component of the net
30 ecosystem C balance, ranging from 2.77 to 7.31 gC/m²/yr. In contrast, four years of continuous

1 Eddy-Covariance (EC)-tower based CO₂ measurements in the birch forest revealed very variable
2 C sink/source functionality, which in two out of four years has been found to be a C source to the
3 atmosphere (Heliasz, 2012). Tundra heath, another important landcover type in this region, has
4 lower C uptake (Christensen et al., 2007; Fox et al., 2008) and both birch forest and tundra heath
5 were found to have high spatial heterogeneity (Fox et al., 2008; Heliasz, 2012). Altogether,
6 different landcover types show diverse contributions to this subarctic ecosystem's C balance.
7 With pronounced future warming expected in this region, the structure and function of the
8 different vegetation types are expected to vary dramatically as has been observed during
9 warming in the recent past (Callaghan et al., 2013). In addition, changes to soil conditions due to
10 warming and permafrost thaw will likely stimulate C fluxes to the atmosphere and affect the
11 long-term accumulated C (Wolf et al., 2008a; McGuire et al., 2012), but this likely C release
12 needs to be weighed against the possibility of increased uptake by increased primary productivity
13 resulting from longer growing seasons and/or potential CO₂ fertilization.

14 The field measurements described above provide an insight into the ongoing processes and
15 current ecosystem status, but until now, no modeling exercises have been implemented in this
16 region in combination with the comprehensive measured data. Moreover, high spatial resolution
17 predictions of future potential dynamics of both vegetation and soil processes and their responses
18 to the projected climate are lacking in this region. In this study, therefore, we aim to assess the
19 Stordalen catchment C budget in a retrospective as well as in a prognostic way by implementing
20 a process-based dynamic ecosystem model (Smith et al., 2001; Miller and Smith, 2012)
21 integrated with a distributed hydrology model (Tang et al., 2014a; Tang et al., 2014b) at high
22 spatial resolution (50 m by 50 m, (Yang et al., 2012)). We quantify the overall C budget of the
23 study catchment by synthesizing diverse C fluxes and specifically address the following
24 questions: (1) Will this subarctic catchment become a C source or a larger C sink in the near
25 future? (2) How differently will the catchment's vegetation micro-types respond to the climate
26 drivers? And (3) what are the major limitations in the model's prognostic ability?

27 To answer these questions, we implemented an Arctic-enabled version of the dynamic ecosystem
28 model, LPJ-GUESS WHyMe (Wania et al., 2009a, 2009b, 2010). This model has been widely
29 and successfully implemented for estimating and predicting ecosystem function in high-latitude
30 regions (McGuire et al., 2012; Miller and Smith, 2012; Zhang et al., 2013). LPJ-GUESS

1 WHyMe includes comprehensive process descriptions to capture the interactions between
2 atmosphere-vegetation-soil domains and it explicitly describes permafrost and peatland
3 processes, which are important components of our study catchment. Importantly, previous
4 studies (Tang et al., 2014a; Tang et al., 2014b) dedicated to integrate a distributed hydrology
5 scheme to LPJ-GUESS WHyMe have demonstrated the necessity of considering lateral water
6 movements to accurately capture water and C cycling in this region. The model with distributed
7 hydrology is called LPJG-WHyMe-TFM where TFM stands for “Triangle Form-based Multiple
8 flow algorithm” (Pilesjö and Hasan, 2014). The study presented here is the first modeling
9 exercise to combine all the available year-around measured data in the Stordalen catchment and
10 at high spatial resolution.

11

12 **2 Model descriptions**

13 The process-based dynamic ecosystem model, LPJG-WHyMe-TFM, was chosen as the platform
14 for studying the subarctic catchment C balance. The processes in the model include vegetation
15 growth, establishment and mortality, disturbance, competition between plant individuals for light
16 and soil water (Smith et al., 2001; Smith et al., 2014) and soil biogeochemical processes (Sitch et
17 al., 2003). These processes are operated in a number of independent and replicate patches.
18 Vegetation in the model is defined and grouped by plant function types (PFTs), which are based
19 on plant phenological and physiognomical features combined with bioclimatic limits (Hickler et
20 al., 2004; Wramneby et al., 2008). Bioclimatic conditions determine which PFTs can potentially
21 grow in study regions, and vertical stand structure together with soil water availability further
22 influence PFT establishment based on PFTs’ shade and drought tolerance characteristics. A list
23 of the simulated PFTs in this catchment can be found in the Supplement, Table S1. The
24 parameterization and choice of non-peatland PFTs in this study cover all the main vegetation
25 types found in the study region (boreal forest, shrubs, open-ground grasses, peatland mosses and
26 flood-tolerant C3 graminoids) and are based on previous studies for the arctic region using LPJ-
27 GUESS (Wolf et al., 2008a; Hickler et al., 2012; Miller and Smith, 2012; Zhang et al., 2013).
28 For peatland grid cells, two new peatland PFTs, flood-tolerant graminoids and *Sphagnum* moss,
29 are introduced by Wania et al. (2009b).

1 The model is driven by monthly/annual climate data and includes both non-peatland and
2 peatland hydrological processes (Fig. 1). The vertical water movement between atmosphere,
3 vegetation and soil is based on Gerten et al. (2004) while the lateral water movement between
4 grid cells was implemented by Tang et al. (2014b) based on topographical variations. More
5 recently, an advanced multiple flow algorithm TFM (Pilesjö and Hasan, 2014) was chosen to
6 distribute water among grid cells, due to its better treatment of flow continuity and flow
7 estimation over flat surfaces (Tang et al., 2014a). Within the catchment boundary, surface and
8 subsurface runoff can move from one upslope cell to multiple downslope cells, which greatly
9 improves hydrological flux estimations (Tang et al., 2014a) and results in a better estimate of C
10 fluxes in peatland region. The soil temperature estimation is driven by surface air temperature,
11 and the Crank-Nicolson heat diffusion algorithm (Crank and Nicolson, 1996) is implemented to
12 calculate the soil temperature profile on a daily time-step (Wania et al., 2009a). The C cycling
13 descriptions in LPJG-WHyMe-TFM for peatland cells are based on Wania's developments
14 (Wania et al., 2009a, 2009b, 2010), while the non-peatland grid cell C cycling is kept the same as
15 in LPJ-GUESS (Smith et al., 2001; Sitch et al., 2003). The full hydrological processes and
16 peatland C cycling descriptions in LPJG-WHyMe-TFM can be found in the Supplement, Text S1.
17 A brief summary of relevant C cycling processes in the model will be presented below.

18 A modified Farquhar photosynthesis scheme (Haxeltine and Prentice, 1996; Haxeltine et al.,
19 1996; Sitch et al., 2003) is used to estimate gross primary production (GPP), which is related to
20 air temperature (T), atmospheric CO₂ concentration, absorbed photosynthetically active radiation
21 (PAR) and stomatal conductance. Part of the GPP is respired to the atmosphere by maintenance
22 and growth respiration (R_a), and the remaining part is net primary production (NPP) for each
23 PFT. The reproduction costs are subtracted from NPP, and thereafter the remaining NPP is
24 allocated to different living tissues in accordance with a set of PFT-specific allometric
25 relationships (Smith et al., 2001). Leaves, fine root biomass and root exudates are transferred to
26 the litter pool with a given turnover rate, and above-ground plant materials can also provide
27 inputs to the litter pool due to stochastic natural disturbance events and mortality (Smith et al.,
28 2001; Thonicke et al., 2001). The majority (70%) of the litter is respired as CO₂ directly to
29 atmosphere, with a fixed fraction entering into fast- and slow-turnover soil organic pools (fSOM
30 and sSOM) (Sitch et al., 2003). The overall decomposition rate in the model is strongly

1 influenced by soil temperature and moisture (Sitch et al., 2003). Additionally, the model also
2 estimates emissions of biogenic volatile organic compounds (BVOC) per PFT (Arneth et al.,
3 2007; Schurgers et al., 2009). However, the modelled BVOC values are not compared in the
4 current study, because they only represent a very small fraction of the modelled NEE and,
5 additionally, there are insufficient growing season measurement data in the study domain to
6 evaluate model performance. The major C cycling pathways can be found in the solid line-box
7 area of Fig. 1. For peatland cells, an extra potential C pool for methanogens (C_{CH_4}) has been
8 added (see dashed line-box area in Fig. 1) and mainly includes root exudates and easily-
9 decomposed materials (Wania et al., 2010). The majority of C_{CH_4} is located in the acrotelm layer
10 (Supplement, Text S1) and the oxidation and production of CH_4 together determine the net
11 emission of CH_4 . In the model, the oxidation of CH_4 through methanotrophic bacteria is turned
12 into CO_2 , whereas the un-oxidized CH_4 can be released to the atmosphere by plant-transport,
13 diffusion and ebullition (see the lines with a solid arrow in Fig. 1). The oxidation level is mainly
14 determined by the location of water table position (*WTP*) in the model (Wania et al., 2010).

15 The biomass production in the current version of LPJ-GUESS WHyMe has no representation of
16 nitrogen (N) limitation and neither N fluxes nor C-N interactions are included (Sitch et al., 2007).
17 The latest version of LPJ-GUESS does include N cycling and N limitation on plant production
18 (Smith et al., 2014), but this capability has not yet been integrated with the customized arctic
19 version of the model adopted in the present paper. Moreover, processes determining
20 concentrations of DOC and DIC in soil water have not yet been explicitly described in the model
21 (Fig. 1). To cover the majority of dissolved C losses and gains in our assessment of the
22 catchment C budget, DOC is estimated by combining modelled runoff with observed DOC
23 concentrations. Measured DIC export data is used directly, based on observations by Olefeldt et
24 al. (2013).

25

1 3 Study site and materials

2 3.1 Stordalen Catchment

3 The Stordalen catchment, located in the discontinuous permafrost region, is situated around 9.5
4 km east of the Abisko Naturvetenskapliga Station (ANS, Abisko Research Station, 68°20'N,
5 19°03'E). The catchment, covering around 16 km², has a steep topography on the southern part
6 and turns into the lower flat peatland region to the north (Fig. 2b). The mean air temperature
7 obtained from ANS records was -0.7°C for the period 1913-2002 (Christensen et al., 2004) and
8 0.49°C for the period 2002-2011 (Callaghan et al., 2013). Climate details of the two warming
9 periods in 20th century are given in Callaghan et al. (2010). The Stordalen catchment is
10 composed of birch forest, tundra heath, peatland, lakes and rivers. Permafrost is only found in
11 the palsa and recent permafrost loss and conversion of palsa into non-permafrost *Eriophorum*
12 sites have been related to the observed warming trends in the region (Åkerman and Johansson,
13 2008). The *Sphagnum* sites have a variable active layer depth and are dominated by *Sphagnum*
14 spp. (PFT: pmoss), while the *Eriophorum* sites are dominated by flood-tolerant *Eriophorum* spp.
15 (PFT: WetGRS). Birch forest (PFT: IBS, *Betula pubescens* ssp. *czerepanovii*), which forms the
16 tree line in this region, is mainly distributed around and to the south of the peatlands and extends
17 upwards to mountain slope areas (Fig. 2). Above the birch tree line, there are extensive areas of
18 sub-arctic ericaceous dwarf-shrub heath dominated by the evergreen species *Vaccinium vitis-*
19 *idaea* and the deciduous species *V. uliginosum* and *V. myrtillus*. Willow shrubs (*Salix* spp.) and
20 dwarf birch shrubs (*Betula nana*) occur at the fringes of the forest and in wetter areas above tree
21 line. The heath shrub species also occur as a ground layer in the forest (see Callaghan et al. (2013)
22 for details of vegetation distribution and changes). Around 5% of the catchment is covered by
23 lakes or small rivers (Lundin et al., 2013). A detailed description of catchment hydrological
24 conditions can be found in Olefeldt et al. (2013). The map in Fig. 2a is based on an object-based
25 vegetation analysis in this area (Lundin et al., submitted). The classification is based on an aerial
26 imagery dataset collected in August 2008, with a spatial resolution of 0.08 by 0.08 meters.

1 **3.2 Model inputs and modelling protocol**

2 **3.2.1 Model inputs**

3 Monthly climate data at 50 m resolution, including temperature, precipitation, and cloudiness,
4 together with annual CO₂ concentration were used to drive the model from 1913 to 2080 for the
5 Stordalen catchment. The detailed descriptions of data sources for the period of 1913-2010 can
6 be found in Tang et al. (2014b). The high spatial resolution of monthly temperature for the
7 period 1913-2000 was developed by Yang et al. (2011) covering the whole catchment, while
8 precipitation and cloudiness were extracted and interpolated from the Climatic Research Unit 1.2
9 dataset (Mitchell et al., 2004). For the period 2001-2012, we obtained 12 years of observed
10 temperature and precipitation data from ANS and interpolated these data to the whole region
11 (Olefeldt et al., 2013). The annual CO₂ concentrations from 1913-2010 were obtained based on
12 McGuire et al. (2001) and TRENDS (<http://cdiac.esd.ornl.gov/trends/co2/contents.htm>). The
13 model was spun up in order to achieve vegetation and C pools in equilibrium with the climate at
14 the beginning of the study period by using the first 30 years of climate forcing data to repeatedly
15 drive the model for 300 years. To run the model into the future, the monthly anomalies of
16 simulation outputs from the Rossby Centre Atmosphere Ocean (RCAO) regional climate model
17 (Koenigk et al., 2011) for the grid cell nearest Stordalen were estimated and applied to the
18 historical datasets at 50 m, assuming the same anomaly for all cells in the study region. RCAO
19 climate data was downscaled for an arctic domain using boundary forcing from a general
20 circulation model forced by emissions from the SRES A1B scenario for the period 2013-2080
21 (Zhang et al., 2013).

22 A soil map provided by the Geological Survey of Sweden was used to identify the peatland
23 fraction of each cell. Notably, the detailed rock area shown in Fig. 2a is not represented by the
24 soil map used. Imagery Digital Elevation Model (DEM) from the National Land Survey of
25 Sweden was used and the TFM algorithm (written in a Matlab script, (R2012)) was used to
26 calculate topographic indices (Pilesjö and Hasan, 2014) used in the model LPJG-WHyMe-TFM.

1 **3.2.2 Additional model parameterization and sensitivity testing**

2 An artificially-adjusted snow density (100 kg/m^3 , following the measurements ranges provided
3 in Judson and Doesken (2000)) was implemented for birch forests to mimic deeper trapped snow
4 in the forest. The observed thick top organic soil in the birch forest (Heliasz, 2012) is also
5 represented in the model by increasing the organic fraction of the top 0.1 m soil layer (Olefeldt
6 and Roulet, 2014) in the model. Additionally, the model simulation uses a single replicate patch
7 in each 50 m grid cell. Finally, an additional simulation was performed in which we kept the CO_2
8 concentration constant after 1960 and allow the remaining inputs to vary as normal to diagnose
9 the extent to which the CO_2 concentration influences on ecosystem dynamics and C fluxes.

10 **3.3 Model evaluation data**

11 The observations used to evaluate the model include: (1) EC-tower measured CO_2 NEE covering
12 the palsa and *Sphagnum* sites during 2008 and 2009 (Olefeldt et al., 2012). (2) EC-tower
13 measured CO_2 NEE at the *Eriophorum* site from 2006-2008 (Christensen et al., 2012); (3) Two
14 years (2006-2007) of EC-tower measured CH_4 fluxes at the *Eriophorum* site (Jackowicz-
15 Korczyński et al., 2010); (4) Analyzed DOC concentrations at the palsa/*Sphagnum* site and
16 *Eriophorum* site from 2008 (Olefeldt and Roulet, 2012); (5) Measured DIC export and DOC
17 concentration at six sampling points from 2007-2009 (Olefeldt et al., 2013); (6) EC-tower
18 measured birch forest CO_2 NEE for four continuous years, 2007–2010 (Heliasz, 2012); (7)
19 Catchment-level annual CO_2 and CH_4 emission from lakes and streams from 2008-2011 (Lundin
20 et al., 2013).

21 **3.4 Calculation of the catchment carbon budget**

22 The catchment level C budget was calculated using estimated C fluxes (CF_i) (after first
23 accounting for observed DOC or DIC fluxes, where available) weighted by landcover fractions
24 (f_i in Eq. (1)). The symbol i in Eq. (1) represents different landcover types, in our case, birch
25 forest, peatland (*Sphagnum* and *Eriophorum* sites), tundra heath and lake/river. To identify the
26 temporal variations of C fluxes, the identification different landcover (except peatland region) is
27 based on the dominant PFTs for each grid cell during the reference period of 2001-2012.

1 Additionally, the aerial photo-based classification of different peatland types is also used when
2 estimating peatland fluxes as a whole (Olefeldt et al., 2012).

$$3 \quad C_{all} = \sum_{i=1}^{i=5} CF_i * f_i \quad (1)$$

4

5 **4 Results**

6 The modelled C fluxes for birch forest, peatland and tundra heath are first compared with the
7 measured data for the period of observation. The seasonality and magnitudes of the fluxes are
8 evaluated and then used to estimate the catchment-level C budget. The modelled long-term C
9 dynamics during the period 1913-2080 are then presented for different landcover types and the
10 catchment-level C budget considering all the available C components is also assessed.

11 **4.1 Evaluation of the carbon balance in the historical period**

12 **4.1.1 Peatland**

13 Both the plant communities and hydrological conditions in the peatland differ among the *palsa*,
14 *Sphagnum* and *Eriophorum* sites. Notably, the measured NEE (see grey bars in Fig. 3a,b) covers
15 both dry hummock (*palsa*) and semi-wet (*Sphagnum* site) vegetation (Olefeldt et al., 2012),
16 whereas our model cannot represent the dry conditions of the *palsa*. Therefore, the observed
17 fluxes over both *palsa* and *Sphagnum* sites were compared with the modelled fluxes at the
18 *Sphagnum* site. The C fluxes magnitudes (including both wintertime emission and summertime
19 uptake) are larger at the *Eriophorum* site, when compared with the *palsa/Sphagnum* site for both
20 measured and modelled data. The modelled NEE at both sites generally captures the seasonality
21 and magnitude of measured NEE, from being a strong sink (negative NEE) of CO₂ during the
22 summer (mainly June-August) to being a wintertime CO₂ source. However, the model is unable
23 to fully capture the C source/sink functionality in September at both sites. Furthermore, the
24 modelled winter respiration at the *Eriophorum* site is very close to the observations, though the
25 model overestimates the wintertime emissions at the *palsa/Sphagnum* site. The mean annual
26 cumulative NEE reveals that the model estimations of C fluxes for both parts of the peatland are

1 within the observed ranges, though with around 20% of underestimation in the three-year
2 averaged annual uptake ($-39.76 \text{ gC/m}^2/\text{yr}$ and $-50.18 \text{ gC/m}^2/\text{yr}$ for the modelled and observed
3 fluxes at the *palsa/Sphagnum* site; $-71.54 \text{ gC/m}^2/\text{yr}$ and $-90.34 \text{ gC/m}^2/\text{yr}$ for the modelled and
4 observed fluxes at the *Eriophorum* site). For the *Eriophorum* site, the three-year mean growing
5 season uptake of C is underestimated by the model (Fig. 3d), which indicates that the modelled
6 photosynthetic rates may be too low, or summer respiration rates may be too high, or both.

7 Two full years (2006 and 2007) of EC-tower measured CH_4 emissions were used to evaluate
8 modelled estimations, and three different pathways of modelled CH_4 are also presented (Fig.
9 3e,f). The seasonal variability is well-described by the model and the modelled cumulative CH_4
10 over the year shows accurate representation of CH_4 emissions when compared with the
11 observations (20.23 and $22.57 \text{ gC/m}^2/\text{yr}$ for the measured and modelled, respectively).
12 Specifically, the wintertime emissions are slightly underestimated but this underestimation is
13 compensated by the overestimated summer emissions. Plant-mediated transport of CH_4
14 dominates during the growing season, while the ebullition and diffusion transport reach a
15 maximum in August. Additionally, the plant-mediated CH_4 emission is the main pathway active
16 during the late spring and early autumn.

17 **4.1.2 Birch forest**

18 The modelled average LAI for the birch forest and understory vegetation is around 1.4 and 0.3,
19 respectively, which are consistent with observations made in this area (Heliasz, 2012). Modelled
20 and measured monthly and cumulative NEE are compared for the years 2007-2010 in Fig. 4.
21 From the monthly NEE comparisons (Fig. 4a), we see that the model underestimates ecosystem
22 respired C both before and after the growing season. The maximum photosynthesis-fixed C in
23 July is lower than that measured for the year 2007-2009, but not for the year 2010. The
24 comparisons in Fig. 4b clearly show the cumulative discrepancies between the modelled NEE
25 and the observations. The years 2009 and 2010 become C sources over the year (with the
26 average annual NEE value of $26.77 \text{ gC/m}^2/\text{yr}$), even though the measured air temperature for the
27 winter and spring is relatively lower than for the years 2007 and 2008 (mean air temperature for
28 all months apart from Jun-Sep is -3.11°C , -3.56°C , -4.26°C , -5.75°C for the years 2007, 2008,
29 2009 and 2010, respectively). The abrupt emergence of strong respiration in 2009 and 2010 is

1 not captured by the model. Furthermore, a comparison of the measured and modelled cumulative
2 NEE reveals that the main discrepancy occurs for the winter fluxes. As seen in Fig. 4b, the
3 observed birch forest cumulative CO₂ emissions from Jan to May reaches 50 gC/m², a value
4 which exceeds the range of the model's predictions. Furthermore, the observed CO₂ fluxes in
5 September indicate a C source but the modelled fluxes are close to zero.

6 The red-shaded areas in Fig. 4a reveal high spatial variations during the growing season and the
7 accumulated variations over the year (the average monthly standard deviations of the four years,
8 see Fig. 4b) demonstrate a remarkable spatial variability of the model-estimated annual NEE.
9 Interestingly, the observed mean annual NEE in both 2007-2008 and 2009-2010 fall within the
10 wide spatial variations indicated by the model.

11 **4.1.3 Tundra heath**

12 Around 29.8% of the catchment with alpine terrain was covered by heaths and dwarf shrubs
13 during the reference period 2001-2012. The model predicts that low-growing evergreen shrubs
14 (PFT: LSE, e.g. *Vaccinium vitis-idaea*) currently dominate in this area, with tall summer-green
15 shrub (PFT: HSS, e.g. *Salix* spp.) dominant in the future predictions (2051-2080) (Fig. 5). Since
16 there is no available year-around observations of the C balance in this part of the Stordalen
17 catchment, a synthesis of published data from similar environments is used to evaluate the model
18 estimations (Table 1).

19 Four periods with averaged C uptake values from our model are presented (see the last four
20 columns in Table 1) and a clear increase of summer uptake can be found with increased
21 temperature and CO₂ concentration. The modelled, whole-year uptake also follows the
22 increasing trend, except for the period of 2051-2080. The model-estimated summer C uptake is
23 much stronger than the observations made at the high arctic heath of NE Greenland, which is
24 reasonable when considering the longer growing season in our catchment. The study conducted
25 in an alpine area in Abisko by Fox et al. (2008) shows a wide range of estimated NEE over 40
26 days during the summer time of 2004. The wide range of NEE values are because three levels of
27 vegetation coverage were studied and the lowest uptake is from sparse vegetation dominated by
28 bare rock and gravels, which is similar to the situation in our tundra heath sites (Fig. 2a). The
29 modelled summer NEE between the years of 2001-2012 integrates the whole summer season

1 (longer than 40 days), and falls within the observed ranges presented by Fox et al. (2008), with
2 values slightly higher than the lowest observed values.

3 **4.1.4 Aquatic systems**

4 • **Lateral waterborne C fluxes**

5 The modelled DOC exports based on runoff estimations are compared with the measured DOC
6 fluxes. The model generally underestimated annual runoff (the measured and modelled mean
7 annual runoff for six points are 279.65 mm and 207.75 mm, respectively), but the modelled
8 accuracy varies from point to point as well as for different years (Tang et al., 2014a). The
9 average DOC export of the birch forest over three years across sampling sites from 2007 to 2009
10 are 3.65, 2.77, and 2.33 gC/m²/yr from the observations and 3.09, 2.03, and 1.69 gC/m²/yr from
11 the model estimations, respectively. The downward trend over the three years is captured and is
12 related to lower precipitation during the latter years. The observed DOC export rates at the
13 *palsa/Sphagnum* and *Eriophorum* sites in 2008 are directly used to represent different types of
14 peatland export level and the values are 3.35 and 7.55 gC/m²/yr for the *palsa/Sphagnum* and
15 *Eriophorum* sites, respectively (Olefeldt and Roulet, 2012). DIC export is currently beyond the
16 scope of our model but nonetheless contributes to the whole C budget. We used an averaged DIC
17 export value of 1.22 gC/m²/yr based on the published data in Olefeldt et al. (2013) and DIC
18 export is included in the estimation of the catchment C budget below (see Table 2).

19 • **Carbon fluxes from Lakes and streams**

20 Investigations of aquatic system C emission in the Stordalen catchment were conducted by
21 Lundin et al. (2013) during the years 2008-2011. Around 5% of the total catchment area (0.75
22 km²) is classified as aquatic systems, with lakes accounting for 96% of the aquatic area. Both
23 lakes and streams contribute to the emissions of CH₄ and CO₂, but the streams dominate CO₂
24 emission while the lakes dominate CH₄ emissions. Averaging across the catchment area, the
25 measured annual CO₂ and CH₄ emissions from streams are 10.1 and 0.06 gC/m²/yr, respectively,
26 while the lake emitted 0.5 gC/m²/yr as CO₂ and 0.1 gC/m²/yr as CH₄ (Lundin et al., submitted).

1 Since river and lake processes are at present beyond the scope of the model, the contribution of
2 aquatic systems to the catchment C fluxes is purely based on the observed data (see Table 2).

3 **4.2 Modelled whole-catchment carbon balance**

4 One of the benefits of using a dynamic vegetation model is that it allows us to investigate the
5 vegetation and C budget responses to climate change. In this section, annual variations of both
6 climate variables (temperature and precipitation) and different ecosystem C fluxes are presented
7 for the whole simulated period. In addition, the normalized catchment C budget is also estimated.

8 Our simulation results suggest that the temperature increase (around 2°C, see Fig. 6, 1a-1c)
9 together with a CO₂ increase to 639 ppm by 2080 could greatly increase the productivity of the
10 birch forest (Fig. 6, 2a-2c and Fig. 5) as well as peatland CH₄ emissions (see Fig. 6, 6a-6c). The
11 DOC export from birch sites also increases slightly over the study period (Fig. 6, 3a-3c). Besides
12 leading to an increase in ecosystem biomass in grid cells currently occupied by birch forest (Fig.
13 5c,d), warming will also result in the current tundra heath close to the birch treeline being
14 replaced by an upward expansion of the birch forest (Fig. 5a,b). This is indicated by the changes
15 to birch treeline's uppermost elevation in Fig. 6, 8a-8c. The dramatic increase of C uptake in the
16 tundra heath region (Fig. 6, 5a-5c) is largely a result of this vegetation succession. Meanwhile,
17 the successive degradation of permafrost and slightly higher annual precipitation may result in
18 more anaerobic conditions for the modelled peatland. Combined with warmer soil conditions,
19 these result in both higher decomposition rates of soil organic matter and greatly increased CH₄
20 production. Moreover, a stronger response of respiration than NPP to the temperature increase
21 reduces the net C uptake in the peatland (see Fig. 6, 4a-4c). The catchment, as a whole, shows an
22 increased C uptake (see the trend line in Fig. 6, 7a) over the 1913-2080 period. The averaged C
23 budgets for the two selected periods (1961-1990 and 2051-2080) are -1.47 and -11.23 gC/m²/yr,
24 respectively, with the increase being dominated by the large increase seen in the uptake rates at
25 the birch forest and tundra heath sites.

26 During the 2051-2080 period, both boreal needle-leaf shade-tolerant spruce (PFT: BNE, e.g.
27 *Picea abies*) and boreal needle-leaf (but less shade-tolerant) pine (PFT: BINE, e.g. *Pinus*
28 *sylvestris*) start to appear in the birch-dominated regions (Fig. 5). In the current tundra regions,

1 the coverage of HSS greatly increases at the expense of LSE. For the northern parts of the
2 catchment, birch forest densification is observed with future warming, while the greatest relative
3 changes in biomass occur near the treeline. The increased temperature together with increased
4 CO₂ concentration by 2080 are very likely to increase CO₂ uptake in both tundra heath and
5 forested areas, though the nutrient limitations are not included in this version of the model (but
6 see (Smith et al., 2014)). A summary of the modelled catchment C components and C fluxes
7 from different sources is given in Table 2. Additionally, the modelled estimations during the
8 warm period of 2000-2005 are also presented in Table 2 and the positive mean value of
9 catchment C-budget is seen to be an exception with reference to the main reference period.
10 Furthermore, the annual variations of the modelled C fluxes in different periods are also
11 presented in Table 2. We find that different landcover types could shift rapidly from being a C
12 sink to a C source in the future (see the mean plus one s.d. value).

13 To illustrate the impact of CO₂ increases alone on the modelled C budget, the differences
14 between simulations (ΔC fluxes) with and without a CO₂ increase since 1960 are shown in Fig. 7.
15 The original outputs of those two simulations are plotted separated in the Supplement, Fig. S1,
16 together with the statistical significance values (p). Interestingly, the simulation with constant
17 CO₂ forcing after 1960 significantly reduces the birch and tundra uptake (positive values in Fig.
18 7), whereas the peatland NEE and CH₄ are not strongly influenced by the CO₂ increase. The
19 catchment C budget dynamics are consistent with the changes seen in the birch and tundra heath
20 regions. Furthermore, the magnitudes of ΔC fluxes for the birch and tundra NEE show an
21 increasing trend after 1971, which is also seen in the ΔC fluxes for the annual GPP and
22 respiration (see birch forest site in Fig. 7(a). Since tundra heath shows the similar trend as birch
23 forest, it is not presented in the figure). However, the relative differences of ΔC fluxes for the
24 annual GPP and ecosystem respiration widen over time, which indicates a stronger response of
25 GPP to the increased CO₂ concentration than ecosystem respiration.

26 To account for the fact that CH₄ is a more potent greenhouse gas than CO₂, an estimation of the
27 global warming potential (GWP) of the two simulations can be made. Assuming the relative
28 climate impact of CH₄ is 28 times greater than CO₂ over a 100 year period (IPCC, 2013), the
29 calculated GWP for the simulation with atmospheric CO₂ increase is three times larger in the
30 period 1961-1990 (27.3 g CO₂-eq) than the period 2051-2080 (8.8 g CO₂-eq). However, in the

1 simulation without CO₂ increase, the GWP in 1961-1990 (40.7 g CO₂-eq) is approximately half
2 of the GWP value for the 2051-2080 period (93.3 g CO₂-eq). This shows that the change in
3 global warming potential found in the model simulations is strongly influenced by the CO₂
4 concentration used to force the model, as the CO₂ trajectory can alter the balance between the
5 GWP changes resulting from C uptake in the birch forest and tundra, and the peatland CH₄
6 emissions.

7

8 **5 Discussion**

9 To our knowledge, our model simulation is the first attempt to create a C budget of a subarctic
10 catchment based on a dynamic global vegetation model applied at the local scale and to predict
11 its evolution in response to a changing climate. The C budget estimations in this paper include
12 major flux components (CO₂, CH₄ and hydrological C fluxes) based on a process-based approach.
13 The magnitude and seasonality of modelled C fluxes compare well with the measurements (Figs
14 3, 4 and Table 1 and 2), which gives us confidence in the ability of our model to represent the
15 main processes influencing the C balance in this region. Our hope is that, by using a process-
16 based modelling approach at high spatial resolution, our methodology will be more robust in
17 estimating the C budget in a changing future climate than other budget estimation methods
18 (Christensen et al., 2007; Worrall et al., 2007). In response to a climate warming scenario, our
19 model shows a general increase in the C sink in both birch forest and tundra heath ecosystems,
20 along with greater CH₄ emissions in the catchment (Fig. 6). Integrated over the catchment, our
21 modelled C budget indicates that the region will be a greater sink of C by 2080, though these
22 estimates are sensitive to the atmospheric CO₂ concentration. Nevertheless, the current model
23 set-up and simulations still contain limitations in both the historical estimations and predictions.
24 Below we discuss the model's current performance as well as a few existing limitations, and
25 further propose some potential model developments. Most of the studies referred to below have
26 been conducted specifically in the area near the Stordalen catchment or in other regions with
27 similar environments.

1 **5.1 Modelling carbon fluxes for the historical period**

2 **5.1.1 Peatland CO₂ and CH₄ emission**

3 The model estimations in the peatland demonstrated skill in representing the relative differences
4 of CO₂ fluxes between the palsa/*Sphagnum* site and *Eriophorum* site. The current model version
5 cannot represent the very dry conditions of the palsa due to the acrotelm-catotelm soil structure
6 (Wania et al., 2009a); therefore, the overestimated emissions rates of CO₂ (Fig. 3a,b) are
7 expected when using the modelled fluxes from the *Sphagnum* site to compare with the measured
8 data covering both the palsa and *Sphagnum* sites (Larsen et al., 2007a; Bäckstrand et al., 2010).
9 The cold-season respiration at the *Sphagnum* site can account for at least 22% of the annual CO₂
10 emissions (Larsen et al., 2007a), which is a further reason for the model overestimations.
11 Moreover, at the *Eriophorum* site, the model slightly underestimated summertime uptake, which
12 was found to be related to modelled summer respiration being higher than dark chamber-
13 measured respiration, though with high spatial variations (Tang et al., 2014a).

14 The accurate representations of annual CH₄ emissions at the *Eriophorum* sites reflect the model's
15 improved estimations of both hydrological conditions and dynamic C inputs to the C_{CH₄} pools
16 (Fig. 1). With the inclusion of the distributed hydrology at 50 m resolution (Tang et al., 2014a;
17 Tang et al., 2014b), the lower-lying peatland can receive surface runoff from the upslope regions
18 and the fact that water can rise to a depth of 10 cm above the surface both creates anaerobic
19 conditions in the model and favours the establishment of flood-tolerant graminoid PFTs such as
20 *Carex* spp., which can transport CH₄ to the atmosphere. Under such anaerobic conditions,
21 decomposition rates are restricted and part of the decomposed C becomes CH₄ (Wania et al.,
22 2010). However, the overestimation of CH₄ emissions during summer time is at least partly
23 likely to be linked to the complexity of modelling the ebullition process (Wania et al., 2010).
24 Based on sensitivity testing shown in Wania et al. (2010), the parameter that controls CH₄/CO₂
25 production ratio under anaerobic conditions can strongly impact the ebullition process, so it is
26 important to determine this parameter more accurately in future studies. Nevertheless, it remains
27 the case that excluding the palsa type could result in a general overestimation of CH₄ emission
28 over the whole peatland.

5.1.2 Wintertime carbon fluxes, thickness of organic layer and disturbance in the birch forest

The high wintertime CO₂ fluxes to the atmosphere observed in the birch forest and the underestimations by our model (Fig. 4) highlight the importance of the representation of winter season C fluxes for the birch forest, particularly as winter temperatures are increasing more than summer temperatures (Callaghan et al., 2010). In the model, the respiration rate is linked to soil temperatures and moisture and the underestimated respiration could be attributed to the lower temperatures estimations in the wintertime (covering all months except Jun-Sep) when compared with the observed soil temperature at 5 and 10 cm depth in 2009 and 2010 (the modelled wintertime soil temperatures is around 1.9°C lower than that observed at both depths). Also, the investigations of snow depth insulation influence on soil temperatures and respiratory activity by Grogan & Jonasson (2003) have shown that soil temperatures contributes to the greatest variations in respiratory activity at our birch sites. The birch forest is located on the relatively lower parts of the catchment (Fig. 2) and traps the wind-shifted lighter snow from the upland tundra heath, creating a much thicker snow pack and therefore significantly increasing the soil temperatures (Groendahl et al., 2007; Larsen et al., 2007b; Luus et al., 2013). Snow depth measurements in the Abisko birch and tundra heath sites from March 24th to April 7th, 2009 (<http://www.nabohome.org/cgi-bin/explore.pl?seq=131>) revealed the snowpack in the birch forest was 26.62 cm deeper on average than the snowpack in the tundra heath. The snow density for the birch forest was artificially decreased to 100 kg/m³ in the model in order to increase the snow depth in the absence of a wind-redistribution mechanism in our model, but it is still hard to capture the high soil temperatures as well as high emission rates in winter.

The thickness of organic soil layer is another crucial component controlling birch site respiration in our catchment (Sjögersten and Wookey, 2002; Heliasz, 2012). The thickness of organic soil is most likely connected to the past transformation of the sites from heath to forest and is expected to decrease if birch biomass continues to increase (Hartley et al., 2012; Hartley et al., 2013). Furthermore, Hartley et al. (2012) showed evidence of the decomposition of older soil organic matter during the middle of the growing season and concluded that with more productive forests in the future, the soil stocks of C will become more labile. From a model perspective, faster

1 turnover rates of soil C pools (Sitch et al., 2007) could be used in climate warming model
2 experiments to reflect the accelerated C mobilization in the soil. This could, to some degree,
3 offset the stronger C uptake in the birch forest site in the simulation results shown here. In
4 addition, the current parameterization of the organic fraction in the birch forest may not fully
5 represent the organic horizons in reality soil.

6 The birch forest is cyclically influenced by the outbreak of moths (*E. autumnata*) and an
7 outbreak in 2004 greatly affected the birch forest, resulting in a much lower C uptake than the
8 average (Heliasz et al., 2011). Even though it is assumed that the fluxes during 2007-2010 had
9 returned to the pre-defoliation levels (*M. Heliasz*, personal communication), it is still difficult to
10 completely exclude the influence of insect disturbance in this forest. For the current model
11 simulation, stochastic mortality and patch-destroying disturbance events have been included to
12 account for the impacts of these random processes on ecosystem C cyclings. However, to give a
13 more accurate and reliable representation of the C fluxes in the birch forest, an explicit
14 representation of insect impacts, outbreaks and their periodicity should be included (Wolf et al.,
15 2008b) as well as other disturbances (Callaghan et al., 2013; Bjerke et al., 2014). For example, a
16 warm event in winter 2007 caused a 26% reduction in biomass over an area of over 1424 km² in
17 summer 2008 (Bokhorst et al., 2009).

18 **5.1.3 Benefits of high spatial resolution and limitations from monthly** 19 **temporal resolution**

20 Subarctic ecosystems are characterized by small-scale variations in vegetation composition,
21 hydrological conditions, nutrient characteristics and C fluxes (Lukeno and Billings, 1985;
22 McGuire et al., 2002; Callaghan et al., 2013). The spatial resolution of 50 m in this model
23 application allowed us to capture the diverse vegetation micro-types and their altitudinal gradient
24 in the catchment, as well as their differential responses to climate changes (Figs. 5 and 6). This is
25 unlikely to be well represented by a simple-averaging approach across the landscape, e.g. RCMs
26 or GCMs. Furthermore, it is worth noting that the carbon cycling in the peatland, especially CH₄
27 fluxes, is sensitive to the *WTP* estimations (Tang et al., 2014a). Without spatially-distinguished
28 climate and topographical data, it becomes impossible to implement our distributed hydrological
29 scheme and thereby capture the peatland *WTP* dynamics. To our knowledge, the use of 50 m

1 climate data as forcing of LPJG-WHyMe-TFM (Yang et al., 2011) is among the most detailed
2 and comprehensive modelling exercises related to C cycling. Although this study focuses on C
3 cycling, the innovative projects changes of vegetation micro-types at high spatial resolution are
4 relevant to local stakeholders such as conservation managers and reindeer herders.

5 Nevertheless, the high spatial resolution data are currently produced with coarser monthly
6 temporal resolution, which could restrict the model's ability to accurately estimate C fluxes at
7 the start and end of the growing season (Figs. 3 and 4). Due to the dramatic variations of day
8 length at high latitudes, a few days of misrepresenting the starting date of the growing season
9 could significantly alter the estimated plant C uptake (Heliasz, 2012). The daily variations are
10 difficult to capture from the interpolated quasi-daily values used in the model. Indeed, such
11 variations strongly highlight the need for climate forcing at a higher temporal resolution for this
12 region, due to the long daylight duration in summer and short growing seasons.

13 **5.2 Projection uncertainties**

14 A temperature increase of 2°C (Fig. 6) and elevated CO₂ concentrations could greatly increase
15 vegetation growth and thus the C sink of the whole catchment. However, the densification and
16 expansion of birch forest as well as the increased presence of boreal spruce and pine PFTs in our
17 projected period (Fig. 5) could be strongly influenced by reindeer grazing and herbivore
18 outbreaks (Hedenås et al., 2011; Callaghan et al., 2013), even though those detected changes are
19 consistent with other models simulations (Wolf et al., 2008a; Miller and Smith, 2012) and
20 general historical trends (Barnekow, 1999). Furthermore, climate warming may favor the spread
21 of insect herbivores, so an assessment of ecosystem responses to future climate change cannot
22 ignore these disturbances (Wolf et al., 2008b) and also other factors such as winter warming
23 events (Bjerke et al., 2014)

24 Temperature increase results in a larger extent of permafrost degradation in the future.
25 Meanwhile, the increased amount of available water from precipitation and lateral inflow may
26 increase the degree of anoxia and further favors the flood-tolerant WetGRS PFT growth as well
27 as CH₄ production. However, the exact extent of wetting or drying of peatland in the future is
28 still highly uncertain, and the model prediction depends strongly on the climate scenario,

1 permafrost thawing and the resulting balance between increased water availability and increased
2 evapotranspiration. If the peatland drying is large enough, the reduced degree of anoxia could
3 reduce CH₄ emissions in the future (Wrona et al., 2006; Riley et al., 2011). In our case, the
4 peatland, located at the lower part of the catchment, receives water from the southern mountain
5 region, and is more likely to become wetter in the near future in response to the increases in
6 water availability (Wrona et al., 2006). Additionally, the determination of grid cell peat fractions
7 in our simulation is dependent on the current (historical) soil map; therefore, the projections of
8 peatland expansion to non-peatland cells cannot be reflected in the current model predictions.
9 This could bring some additional uncertainties into the catchment C-budget estimations (Malmer
10 et al., 2005; Marushchak et al., 2013).

11 To cover all the major C components in this catchment, the current estimations of the C budget
12 used available, observed aquatic emissions and DOC concentration and DIC export values, all of
13 which were assumed constant for the whole simulation period, 1913-2080. However, the
14 direction and magnitude of changes to aquatic C fluxes are hard to quantify without modelling
15 additional processes in these systems. Previous studies have found that the substantial thawing of
16 permafrost as well as increased precipitation in recent decades have significantly increased total
17 organic carbon (TOC) concentrations in lakes (Kokfelt et al., 2009; Karlsson et al., 2010). The
18 increased loadings of nutrients and sediments in lakes are very likely to increase productivity of
19 aquatic vegetation, but the effects may be offset by the increased inputs from terrestrial organic
20 C and increases in respiration (Wrona et al., 2006; Karlsson et al., 2010). Emissions of CH₄ from
21 aquatic systems are more likely to increase due to the longer ice-free season (Callaghan et al.,
22 2010), increased methanogenesis in sediments and also increased CH₄ transport by vascular
23 plants (Wrona et al., 2006). Furthermore, a recent study by Wik et al. (2014) found that CH₄
24 ebullition from lakes is strongly related to heat fluxes into the lakes. Therefore, future changes to
25 energy fluxes together with lateral transports of dissolved C from terrestrial ecosystems to the
26 aquatic ecosystems are especially important for predicting C emissions from aquatic systems.

27 As we have discussed, the dynamics of birch forest and to a lesser extent tundra heath C
28 assimilation largely determines the catchment's C budget (Figs. 5 and 6), whereas the dramatic
29 increase of CH₄ can slightly offset the net climate impact of the projected C uptake. Furthermore,
30 both modelled C budget and GWP values are very sensitive to the atmospheric CO₂ levels.

1 However, to date, there is no clear evidence showing significant long-term CO₂ fertilization
2 effects in the arctic region (Oechel et al., 1994; Gwynn-Jones et al., 1997; Olsrud et al., 2010).
3 Two possible reasons for this lack of CO₂ fertilization response might be that CO₂ levels close to
4 the moss surface in birch forest can reach as high as 1140 ppm already and are normally within
5 the range of 400-450 ppm (Sonesson et al., 1992) while tall vegetation such as shrubs and birch
6 trees as well as peatland species have not been manipulated by CO₂ fertilization. Over the long-
7 term, vegetation growth is likely a result of complex interactions between nutrient supplies
8 (McNown and Sullivan, 2013), UV-B exposure (Schipperges and Gehrke, 1996; Johnson et al.,
9 2002), temperature and growing season length (Heath et al., 2005) and forest longevity
10 (Bugmann and Bigler, 2011). Therefore, more field experiments are urgently needed in order to
11 quantify and understand the CO₂ fertilization effects on the various vegetation micro-types of the
12 subarctic environment, and particularly tall vegetation types.

13 Overall, the current model application has been valuable in pointing to these gaps in process
14 understanding and meanwhile shows the importance of including vegetation dynamics in studies
15 of C balance. Furthermore, a current inability to include the potential impacts of peatland
16 expansion, potential increases of emissions from aquatic systems as well as the potential nutrient
17 limitations on plants (but see Smith et al. (2014)) and disturbances (Bjerke et al., 2014), make it
18 likely that our projections of the catchment C-budget and CO₂-GWP will vary from those that
19 may be observed in the future. However, our high spatial resolution, process-based modelling in
20 the subarctic catchment provides an insight into the complexity of responses to climate change of
21 a subarctic ecosystem while simultaneously revealing some key uncertainties that ought to be
22 dealt with in future model development. These developments would be aided by certain new
23 observations and environmental manipulations, particularly of CO₂ with FACE experiments of
24 shrubs and trees, in order to improve our understanding and quantification of complex subarctic
25 processes.

26

27 **Acknowledgements**

28 The authors would like to thanks Dr. Rita Wania for providing the original LPJ-WHyMe code.
29 We want to thank Dr. Thomas Holst, Dr. Guy Schurgers and Dr. Anneli Poska for interesting and

1 informative discussions. We thank Ralf Döscher and Torben Koenigk (SMHI) for the providing
2 us with regional climate projection data and anomalies. PAM acknowledges financial support
3 from the ADSIMNOR (Advanced Simulation of Arctic Climate and Impact on Northern Regions)
4 project funded by FORMAS (Swedish Research Council), and the Lund University Centre for
5 the study of Climate and Carbon Cycle (LUCCI) funded by VR. The study is a contribution to
6 the strategic research area Modelling the Regional and Global Earth System (MERGE), the
7 Nordic Centre of Excellence DEFROST and the EU PAGE21 project. TVC and TRC wish to
8 thank FORMAS for funding for the project “Climate change, impacts and adaptation in the sub-
9 Arctic: a case study from the northern Swedish mountains” (214-2008-188) and the EU
10 Framework 7 Infrastructure Project “INTERACT” (www.eu-interact.com).

11

1 **References**

- 2 Åkerman, H. J., and Johansson, M.: Thawing permafrost and thicker active layers in sub-arctic
3 Sweden, *Permafrost and Periglacial Processes*, 19, 279-292, doi:10.1002/ppp.626, 2008.
- 4 AMAP: Arctic Climate Issues 2011: Changes in Arctic Snow, Water, Ice and Permafrost, Oslo,
5 2012.
- 6 Arneeth, A., Niinemets, Ü., Pressley, S., Bäck, J., Hari, P., Karl, T., Noe, S., Prentice, I. C., Serça,
7 D., Hickler, T., Wolf, A., and Smith, B.: Process-based estimates of terrestrial ecosystem
8 isoprene emissions: incorporating the effects of a direct CO₂-isoprene interaction, *Atmos. Chem.*
9 *Phys.*, 7, 31-53, doi:10.5194/acp-7-31-2007, 2007.
- 10 Bäckstrand, K.: Carbon gas biogeochemistry of a northern peatland - in a dynamic permafrost
11 landscape, Doctoral, Faculty of Science, Department of Geology and Geochemistry, Stockholm
12 University, 2008.
- 13 Bäckstrand, K., Crill, P. M., Jackowicz-Korczyński, M., Mastepanov, M., Christensen, T. R., and
14 Bastviken, D.: Annual carbon gas budget for a subarctic peatland, Northern Sweden,
15 *Biogeosciences*, 7, 95-108, doi:10.5194/bg-7-95-2010, 2010.
- 16 Barnekow, L.: Holocene tree-line dynamics and inferred climatic changes in the Abisko area,
17 northern Sweden, based on macrofossil and pollen records, *The Holocene*, 9, 253-265,
18 doi:10.1191/095968399676322637, 1999.
- 19 Bjerke, J. W., Stein Rune, K., Kjell Arild, H., Eirik, M., Jane, U. J., Sarah, L., Dagrún, V.-S., and
20 Hans, T.: Record-low primary productivity and high plant damage in the Nordic Arctic Region in
21 2012 caused by multiple weather events and pest outbreaks, *Environmental Research Letters*, 9,
22 084006, 2014.
- 23 Bokhorst, S. F., Bjerke, J. W., Tømmervik, H., Callaghan, T. V., and Phoenix, G. K.: Winter
24 warming events damage sub-Arctic vegetation: consistent evidence from an experimental
25 manipulation and a natural event, *Journal of Ecology*, 97, 1408-1415, doi:10.1111/j.1365-
26 2745.2009.01554.x, 2009.
- 27 Bugmann, H., and Bigler, C.: Will the CO₂ fertilization effect in forests be offset by reduced tree
28 longevity?, *Oecologia*, 165, 533-544, doi:10.1007/s00442-010-1837-4, 2011.
- 29 Callaghan, T. V., Bergholm, F., Christensen, T. R., Jonasson, C., Kokfelt, U., and Johansson, M.:
30 A new climate era in the sub-Arctic: Accelerating climate changes and multiple impacts,
31 *Geophysical Research Letters*, 37, L14705, doi:10.1029/2009GL042064, 2010.
- 32 Callaghan, T. V., Jonasson, C., Thierfelder, T., Yang, Z., Hedenås, H., Johansson, M., Molau, U.,
33 Van Bogaert, R., Michelsen, A., Olofsson, J., Gwynn-Jones, D., Bokhorst, S., Phoenix, G.,
34 Bjerke, J. W., Tømmervik, H., Christensen, T. R., Hanna, E., Koller, E. K., and Sloan, V. L.:
35 Ecosystem change and stability over multiple decades in the Swedish subarctic: complex
36 processes and multiple drivers, *Philosophical Transactions of the Royal Society B: Biological*
37 *Sciences*, 368, doi:10.1098/rstb.2012.0488, 2013.
- 38 Christensen, T. R., Johansson, T., Åkerman, H. J., Mastepanov, M., Malmer, N., Friberg, T.,
39 Crill, P., and Svensson, B. H.: Thawing sub-arctic permafrost; effects on vegetation and methane
40 emissions, *Geophysical Research Letters*, 31, 2004.
- 41 Christensen, T. R., Johansson, T., Olsrud, M., Strom, L., Lindroth, A., Mastepanov, M., Malmer,
42 N., Friberg, T., Crill, P., and Callaghan, T. V.: A catchment-scale carbon and greenhouse gas
43 budget of a subarctic landscape, *Philosophical Transactions - Royal Society. Mathematical,*
44 *Physical and Engineering Sciences*, 365, 1643-1656, 2007.

1 Christensen, T. R., Jackowicz-Korczyński, M., Aurela, M., Crill, P., Heliasz, M., Mastepanov,
2 M., and Friborg, T.: Monitoring the Multi-Year Carbon Balance of a Subarctic Palsa Mire with
3 Micrometeorological Techniques, *AMBIO*, 41, 207-217, doi:10.1007/s13280-012-0302-5, 2012.
4 Crank, J., and Nicolson, P.: A practical method for numerical evaluation of solutions of partial
5 differential equations of the heat-conduction type, *Adv Comput Math*, 6, 207-226,
6 doi:10.1007/BF02127704, 1996.
7 Fox, A. M., Huntley, B., Lloyd, C. R., Williams, M., and Baxter, R.: Net ecosystem exchange
8 over heterogeneous Arctic tundra: Scaling between chamber and eddy covariance measurements,
9 *Global Biogeochemical Cycles*, 22, GB2027, doi:10.1029/2007GB003027, 2008.
10 Gerten, D., Schaphoff, S., Haberlandt, U., Lucht, W., and Sitch, S.: Terrestrial vegetation and
11 water balance--hydrological evaluation of a dynamic global vegetation model, *Journal of*
12 *Hydrology*, 286, 249-270, doi:10.1016/j.jhydrol.2003.09.029, 2004.
13 Groendahl, L., Friborg, T., and Soegaard, H.: Temperature and snow-melt controls on
14 interannual variability in carbon exchange in the high Arctic, *Theor Appl Climatol*, 88, 111-125,
15 doi:10.1007/s00704-005-0228-y, 2007.
16 Grogan, P., and Jonasson, S.: Controls on Annual Nitrogen Cycling in the Understory of a
17 Subarctic Birch Forest, *Ecology*, 84, 202-218, doi:10.2307/3108009, 2003.
18 Grogan, P., and Jonasson, S.: Ecosystem CO₂ production during winter in a Swedish subarctic
19 region: the relative importance of climate and vegetation type, *Global Change Biology*, 12, 1479-
20 1495, doi:10.1111/j.1365-2486.2006.01184.x, 2006.
21 Gwynn-Jones, D., Lee, J. A., and Callaghan, T. V.: Effects of enhanced UV-B radiation and
22 elevated carbon dioxide concentrations on a sub-arctic forest heath ecosystem, *Plant Ecology*,
23 128, 243-249, doi:10.1023/A:1009771125992, 1997.
24 Hartley, I. P., Garnett, M. H., Sommerkorn, M., Hopkins, D. W., Fletcher, B. J., Sloan, V. L.,
25 Phoenix, G. K., and Wookey, P. A.: A potential loss of carbon associated with greater plant
26 growth in the European Arctic, *Nature Clim. Change*, 2, 875-879, doi:10.1038/nclimate1575,
27 2012.
28 Hartley, I. P., Garnett, M. H., Sommerkorn, M., Hopkins, D. W., and Wookey, P. A.: The age of
29 CO₂ released from soils in contrasting ecosystems during the arctic winter, *Soil Biology and*
30 *Biochemistry*, 63, 1-4, doi:10.1016/j.soilbio.2013.03.011, 2013.
31 Haxeltine, A., and Prentice, I. C.: BIOME3: An equilibrium terrestrial biosphere model based on
32 ecophysiological constraints, resource availability, and competition among plant functional types,
33 *Global Biogeochemical Cycles*, 10, doi:citeulike-article-id:4600877, 1996.
34 Haxeltine, A., Prentice, I. C., and Creswell, I. D.: A Coupled Carbon and Water Flux Model to
35 Predict Vegetation Structure, *Journal of Vegetation Science*, 7, 651-666, 1996.
36 Heath, J., Ayres, E., Possell, M., Bardgett, R. D., Black, H. I. J., Grant, H., Ineson, P., and
37 Kerstiens, G.: Rising atmospheric CO₂ reduces sequestration of root-derived soil carbon, 309,
38 1711-1713, doi:10.1126/science.1110700, 2005.
39 Hedenås, H., Olsson, H., Jonasson, C., Bergstedt, J., Dahlberg, U., and Callaghan, T.: Changes in
40 Tree Growth, Biomass and Vegetation Over a 13-Year Period in the Swedish Sub-Arctic,
41 *AMBIO*, 40, 672-682, doi:10.1007/s13280-011-0173-1, 2011.
42 Heliasz, M., Johansson, T., Lindroth, A., Mölder, M., Mastepanov, M., Friborg, T., Callaghan, T.
43 V., and Christensen, T. R.: Quantification of C uptake in subarctic birch forest after setback by
44 an extreme insect outbreak, *Geophysical Research Letters*, 38, L01704,
45 doi:10.1029/2010GL044733, 2011.

1 Heliasz, M.: Spatial and temporal dynamics of subarctic birch forest carbon exchange, Doctoral,
2 Department of Physical Geography and Ecosystems Science, Lund University Sweden, 132 pp.,
3 2012.

4 Hickler, T., Smith, B., Sykes, M. T., Davis, M. B., Sugita, S., and Walker, K.: Using a
5 generalized vegetation model to simulate vegetation dynamics in northeastern USA, *Ecology*, 85,
6 519-530, doi:10.1890/02-0344, 2004.

7 Hickler, T., Vohland, K., Feehan, J., Miller, P. A., Smith, B., Costa, L., Giesecke, T., Fronzek, S.,
8 Carter, T. R., Cramer, W., Kühn, I., and Sykes, M. T.: Projecting the future distribution of
9 European potential natural vegetation zones with a generalized, tree species-based dynamic
10 vegetation model, *Global Ecology and Biogeography*, 21, 50-63, doi:10.1111/j.1466-
11 8238.2010.00613.x, 2012.

12 IPCC: *Climate Change 2013: The Physical Science Basis*, NY, USA, 2013.

13 Jackowicz-Korczyński, M., Christensen, T. R., Bäckstrand, K., Crill, P., Friborg, T., Mastepanov,
14 M., and Ström, L.: Annual cycle of methane emission from a subarctic peatland, *Journal of*
15 *Geophysical Research: Biogeosciences*, 115, G02009, doi:10.1029/2008JG000913, 2010.

16 Johnson, D., Campbell, C. D., Lee, J. A., Callaghan, T. V., and Gwynn-Jones, D.: Arctic
17 microorganisms respond more to elevated UV-B radiation than CO₂, *Nature*, 416, 82-83,
18 doi:10.1038/416082a, 2002.

19 Jonasson, S., and Michelsen, A.: Nutrient Cycling in Subarctic and Arctic Ecosystems, with
20 Special Reference to the Abisko and Torneträsk Region, *Ecological Bulletins*, 45-52,
21 doi:10.2307/20113182, 1996.

22 Judson, A., and Doesken, N.: Density of Freshly Fallen Snow in the Central Rocky Mountains,
23 *Bulletin of the American Meteorological Society*, 81, 1577-1587, doi:10.1175/1520-
24 0477(2000)081<1577:DOFFSI>2.3.CO;2, 2000.

25 Karlsson, J., Christensen, T. R., Crill, P., Förster, J., Hammarlund, D., Jackowicz-Korczynski,
26 M., Kokfelt, U., Roehm, C., and Rosén, P.: Quantifying the relative importance of lake emissions
27 in the carbon budget of a subarctic catchment, *Journal of Geophysical Research: Biogeosciences*,
28 115, G03006, doi:10.1029/2010JG001305, 2010.

29 Keuper, F., van Bodegom, P. M., Dorrepaal, E., Weedon, J. T., van Hal, J., van Logtestijn, R. S.
30 P., and Aerts, R.: A frozen feast: thawing permafrost increases plant-available nitrogen in
31 subarctic peatlands, *Global Change Biology*, 18, 1998-2007, doi:10.1111/j.1365-
32 2486.2012.02663.x, 2012.

33 Koenigk, T., Döscher, R., and Nikulin, G.: Arctic future scenario experiments with a coupled
34 regional climate model, *Tellus A*, 63, 69-86, doi:10.1111/j.1600-0870.2010.00474.x, 2011.

35 Kokfelt, U., Rosen, P., Schoning, K., Christensen, T. R., FÖRster, J., Karlsson, J., Reuss, N.,
36 Rundgren, M., Callaghan, T. V., Jonasson, C., and Hammarlund, D.: Ecosystem responses to
37 increased precipitation and permafrost decay in subarctic Sweden inferred from peat and lake
38 sediments, *Global Change Biology*, 15, 1652-1663, doi:10.1111/j.1365-2486.2009.01880.x,
39 2009.

40 Koven, C. D., Ringeval, B., Friedlingstein, P., Ciais, P., Cadule, P., Khvorostyanov, D., Krinner,
41 G., and Tarnocai, C.: Permafrost carbon-climate feedbacks accelerate global warming,
42 *Proceedings of the National Academy of Sciences*, doi:10.1073/pnas.1103910108, 2011.

43 Larsen, K. S., Grogan, P., Jonasson, S., and Michelsen, A.: Respiration and Microbial Dynamics
44 in Two Subarctic Ecosystems during Winter and Spring Thaw: Effects of Increased Snow Depth,

1 Arctic, Antarctic, and Alpine Research, 39, 268-276, doi:10.1657/1523-
2 0430(2007)39[268:RAMDIT]2.0.CO;2, 2007a.

3 Larsen, K. S., Ibrom, A., Jonasson, S., Michelsen, A., and Beier, C.: Significance of cold-season
4 respiration and photosynthesis in a subarctic heath ecosystem in Northern Sweden, *Global*
5 *Change Biology*, 13, 1498-1508, doi:10.1111/j.1365-2486.2007.01370.x, 2007b.

6 Lukeno, J. O., and Billings, W. D.: The influence of microtopographic heterogeneity on carbon
7 dioxide efflux from a subarctic bog, *Ecography*, 8, 306-312, doi:10.1111/j.1600-
8 0587.1985.tb01183.x, 1985.

9 Lundin, E. J., Giesler, R., Persson, A., Thompson, M. S., and Karlsson, J.: Integrating carbon
10 emissions from lakes and streams in a subarctic catchment, *Journal of Geophysical Research:*
11 *Biogeosciences*, 118, 1200-1207, doi:10.1002/jgrg.20092, 2013.

12 Luus, K. A., Lin, J. C., Kelly, R. E. J., and Duguay, C. R.: Subnivean Arctic and sub-Arctic net
13 ecosystem exchange (NEE): Towards representing snow season processes in models of NEE
14 using cryospheric remote sensing, *Progress in Physical Geography*, 37, 484-515,
15 doi:10.1177/0309133313491130, 2013.

16 Malmer, N., Johansson, T., Olsrud, M., and Christensen, T. R.: Vegetation, climatic changes and
17 net carbon sequestration in a North-Scandinavian subarctic mire over 30 years, *Global Change*
18 *Biology*, 11, 1895-1909, doi:10.1111/j.1365-2486.2005.01042.x, 2005.

19 Marushchak, M. E., Kiepe, I., Biasi, C., Elsakov, V., Friborg, T., Johansson, T., Soegaard, H.,
20 Virtanen, T., and Martikainen, P. J.: Carbon dioxide balance of subarctic tundra from plot to
21 regional scales, *Biogeosciences*, 10, 437-452, doi:10.5194/bg-10-437-2013, 2013.

22 Mastepanov, M., Sigsgaard, C., Dlugokencky, E. J., Houweling, S., Strom, L., Tamstorf, M. P.,
23 and Christensen, T. R.: Large tundra methane burst during onset of freezing, *Nature*, 456, 628-
24 630, doi:10.1038/nature07464, 2008.

25 McGuire, A. D., Sitch, S., Clein, J. S., Dargaville, R., Esser, G., Foley, J., Heimann, M., Joos, F.,
26 Kaplan, J., Kicklighter, D. W., Meier, R. A., Melillo, J. M., Moore, B., Prentice, I. C.,
27 Ramankutty, N., Reichenau, T., Schloss, A., Tian, H., Williams, L. J., and Wittenberg, U.:
28 Carbon balance of the terrestrial biosphere in the Twentieth Century: Analyses of CO₂, climate
29 and land use effects with four process-based ecosystem models, *Global Biogeochemical Cycles*,
30 15, 183-206, doi:10.1029/2000GB001298, 2001.

31 McGuire, A. D., Wirth, C., Apps, M., Beringer, J., Clein, J., Epstein, H., Kicklighter, D. W.,
32 Bhatti, J., Chapin, F. S., de Groot, B., Efremov, D., Eugster, W., Fukuda, M., Gower, T.,
33 Hinzman, L., Huntley, B., Jia, G. J., Kasischke, E., Melillo, J., Romanovsky, V., Shvidenko, A.,
34 Vaganov, E., and Walker, D.: Environmental variation, vegetation distribution, carbon dynamics
35 and water/energy exchange at high latitudes, *Journal of Vegetation Science*, 13, 301-314,
36 doi:10.1111/j.1654-1103.2002.tb02055.x, 2002.

37 McGuire, A. D., Christensen, T. R., Hayes, D., Heroult, A., Euskirchen, E., Kimball, J. S.,
38 Koven, C., Lafleur, P., Miller, P. A., Oechel, W., Peylin, P., Williams, M., and Yi, Y.: An
39 assessment of the carbon balance of Arctic tundra: comparisons among observations, process
40 models, and atmospheric inversions, *Biogeosciences*, 9, 3185-3204, doi:10.5194/bg-9-3185-2012,
41 2012.

42 McNown, R. W., and Sullivan, P. F.: Low photosynthesis of treeline white spruce is associated
43 with limited soil nitrogen availability in the Western Brooks Range, Alaska, *Functional Ecology*,
44 27, 672-683, doi:10.1111/1365-2435.12082, 2013.

1 Miller, P. A., and Smith, B.: Modelling Tundra Vegetation Response to Recent Arctic Warming,
2 *AMBIO: A Journal of the Human Environment*, 41, 281-291, doi:10.1007/s13280-012-0306-1,
3 2012.

4 Mitchell, T. D., Carter, T. R., Jones, P. D., Hulme, M., and New, M.: A comprehensive set of
5 high-resolution grids of monthly climate for Europe and the globe: the observed record (1901-
6 2000) and 16 scenarios (2001-2100), Tyndall Centre, UEA, Norwich, UK, 2004.

7 Oechel, W. C., Cowles, S., Grulke, N., Hastings, S. J., Lawrence, B., Prudhomme, T., Riechers,
8 G., Strain, B., Tissue, D., and Vourlitis, G.: Transient nature of CO₂ fertilization in Arctic tundra,
9 *Nature*, 371, 500-503, 1994.

10 Olefeldt, D., and Roulet, N. T.: Effects of permafrost and hydrology on the composition and
11 transport of dissolved organic carbon in a subarctic peatland complex, *Journal of Geophysical*
12 *Research G: Biogeosciences*, 117, doi:10.1029/2011jg001819, 2012.

13 Olefeldt, D., Roulet, N. T., Bergeron, O., Crill, P., Bäckstrand, K., and Christensen, T. R.: Net
14 carbon accumulation of a high-latitude permafrost palsa mire similar to permafrost-free
15 peatlands, *Geophysical Research Letters*, 39, L03501, doi:10.1029/2011GL050355, 2012.

16 Olefeldt, D., Roulet, N., Giesler, R., and Persson, A.: Total waterborne carbon export and DOC
17 composition from ten nested subarctic peatland catchments—importance of peatland cover,
18 groundwater influence, and inter-annual variability of precipitation patterns, *Hydrological*
19 *Processes*, 27, 2280-2294, doi:10.1002/hyp.9358, 2013.

20 Olefeldt, D., and Roulet, N. T.: Permafrost conditions in peatlands regulate magnitude, timing,
21 and chemical composition of catchment dissolved organic carbon export, *Global Change Biology*,
22 doi:10.1111/gcb.12607, 2014.

23 Olsrud, M., Carlsson, B. Å., Svensson, B. M., Michelsen, A., and Melillo, J. M.: Responses of
24 fungal root colonization, plant cover and leaf nutrients to long-term exposure to elevated
25 atmospheric CO₂ and warming in a subarctic birch forest understory, *Global Change Biology*, 16,
26 1820-1829, doi:10.1111/j.1365-2486.2009.02079.x, 2010.

27 Pilesjö, P., and Hasan, A.: A Triangular Form-based Multiple Flow Algorithm to Estimate
28 Overland Flow Distribution and Accumulation on a Digital Elevation Model, *Transactions in*
29 *GIS*, 18, 108-124, doi:10.1111/tgis.12015, 2014.

30 Riley, W. J., Subin, Z. M., Lawrence, D. M., Swenson, S. C., Torn, M. S., Meng, L., Mahowald,
31 N. M., and Hess, P.: Barriers to predicting changes in global terrestrial methane fluxes: analyses
32 using CLM4Me, a methane biogeochemistry model integrated in CESM, *Biogeosciences*, 8,
33 1925-1953, doi:10.5194/bg-8-1925-2011, 2011.

34 Roulet, N. T., Lafleur, P. M., Richard, P. J. H., Moore, T. R., Humphreys, E. R., and Bubier, J.:
35 Contemporary carbon balance and late Holocene carbon accumulation in a northern peatland,
36 *Global Change Biology*, 13, 397-411, doi:10.1111/j.1365-2486.2006.01292.x, 2007.

37 Schipperges, B., and Gehrke, C.: Photosynthetic Characteristics of Subarctic Mosses and Lichens,
38 *Ecological Bulletins*, 121-126, doi:10.2307/20113190, 1996.

39 Schurgers, G., Arneth, A., Holzinger, R., and Goldstein, A. H.: Process-based modelling of
40 biogenic monoterpene emissions combining production and release from storage, *Atmos. Chem.*
41 *Phys.*, 9, 3409-3423, doi:10.5194/acp-9-3409-2009, 2009.

42 Sitch, S., Smith, B., Prentice, I. C., Arneth, A., Bondeau, A., Cramer, W., Kaplan, J. O., Levis, S.,
43 Lucht, W., Sykes, M. T., Thonicke, K., and Venevsky, S.: Evaluation of ecosystem dynamics,
44 plant geography and terrestrial carbon cycling in the LPJ dynamic global vegetation model,
45 *Global Change Biology*, 9, 161-185, doi:10.1046/j.1365-2486.2003.00569.x, 2003.

1 Sitch, S., McGuire, A. D., Kimball, J., Gedney, N., Gamon, J., Engstrom, R., Wolf, A., Zhuang,
2 Q., Clein, J., and McDonald, K. C.: Assessing the carbon balance of circumpolar Arctic tundra
3 using remote sensing and process modeling, *Ecological Applications*, 17, 213-234,
4 doi:10.1890/1051-0761(2007)017[0213:ATCBOC]2.0.CO;2, 2007.

5 Sjögersten, S., and Wookey, P. A.: Climatic and resource quality controls on soil respiration
6 across a forest–tundra ecotone in Swedish Lapland, *Soil Biology and Biochemistry*, 34, 1633-
7 1646, doi:10.1016/S0038-0717(02)00147-5, 2002.

8 Smith, B., Prentice, I. C., and Sykes, M. T.: Representation of vegetation dynamics in the
9 modelling of terrestrial ecosystems: comparing two contrasting approaches within European
10 climate space, *Global Ecology and Biogeography*, 10, 621-637, doi:10.1046/j.1466-
11 822X.2001.t01-1-00256.x, 2001.

12 Smith, B., Wårlind, D., Arneth, A., Hickler, T., Leadley, P., Siltberg, J., and Zaehle, S.:
13 Implications of incorporating N cycling and N limitations on primary production in an
14 individual-based dynamic vegetation model, *Biogeosciences*, 11, 2027-2054, doi:10.5194/bg-11-
15 2027-2014, 2014.

16 Sonesson, M., Gehrke, C., and Tjus, M.: CO₂ environment, microclimate and photosynthetic
17 characteristics of the moss *Hylocomium splendens* in a subarctic habitat, *Oecologia*, 92, 23-29,
18 doi:10.1007/BF00317258, 1992.

19 Tagesson, T., Mastepanov, M., Tamstorf, M., Eklundh, L., Schubert, P., Ekberg, A., Sigsgaard,
20 C., Christensen, T., and Ström, L.: Satellites reveal an increase in gross primary production in a
21 greenlandic high arctic fen 1992-2008, *Biogeosciences Discussions*, 7, 2010.

22 Tang, J., Miller, P. A., Crill, P. M., Olin, S., and Pilesjö, P.: Investigating the influence of two
23 different flow routing algorithms on soil–water–vegetation interactions using the dynamic
24 ecosystem model LPJ-GUESS, *Ecohydrology*, doi:10.1002/eco.1526, 2014a.

25 Tang, J., Pilesjö, P., Miller, P. A., Persson, A., Yang, Z., Hanna, E., and Callaghan, T. V.:
26 Incorporating topographic indices into dynamic ecosystem modelling using LPJ-GUESS,
27 *Ecohydrology*, 7, 1147-1162, doi:10.1002/eco.1446, 2014b.

28 Tarnocai, C., Canadell, J. G., Schuur, E. A. G., Kuhry, P., Mazhitova, G., and Zimov, S.: Soil
29 organic carbon pools in the northern circumpolar permafrost region, *Global Biogeochemical*
30 *Cycles*, 23, GB2023, doi:10.1029/2008GB003327, 2009.

31 Thonicke, K., Venevsky, S., Sitch, S., and Cramer, W.: The role of fire disturbance for global
32 vegetation dynamics: coupling fire into a Dynamic Global Vegetation Model, *Global Ecology*
33 *and Biogeography*, 10, 661-677, doi:10.1046/j.1466-822X.2001.00175.x, 2001.

34 Tranvik, L. J., Downing, J. A., Cotner, J. B., Loiselle, S. A., Striegl, R. G., Ballatore, T. J.,
35 Dillon, P., Finlay, K., Fortino, K., Knoll, L. B., Kortelainen, P. L., Kutser, T., Larsen, S., Laurion,
36 I., Leech, D. M., Leigh McCallister, S., McKnight, D. M., Melack, J. M., Overholt, E., Porter, J.
37 A., Prairie, Y., Renwick, W. H., Roland, F., Sherman, B. S., Schindler, D. W., Sobek, S.,
38 Tremblay, A., Vanni, M. J., Verschoor, A. M., Von Wachenfeldt, E., and Weyhenmeyer, G. A.:
39 Lakes and reservoirs as regulators of carbon cycling and climate, *Limnology and Oceanography*,
40 54, 2298-2314, 2009.

41 Van Bogaert, R., Jonasson, C., De Dapper, M., and Callaghan, T. V.: Competitive interaction
42 between aspen and birch moderated by invertebrate and vertebrate herbivores and climate
43 warming, *Plant Ecology & Diversity*, 2, 221-232, doi:10.1080/17550870903487456, 2009.

1 Wania, R., Ross, I., and Prentice, I. C.: Integrating peatlands and permafrost into a dynamic
2 global vegetation model; 1, Evaluation and sensitivity of physical land surface processes, *Global*
3 *Biogeochemical Cycles*, 23, doi:10.1029/2008gb003412, 2009a.

4 Wania, R., Ross, I., and Prentice, I. C.: Integrating peatlands and permafrost into a dynamic
5 global vegetation model; 2, Evaluation and sensitivity of vegetation and carbon cycle processes,
6 *Global Biogeochemical Cycles*, 23, doi:10.1029/2008gb003413, 2009b.

7 Wania, R., Ross, I., and Prentice, I. C.: Implementation and evaluation of a new methane model
8 within a dynamic global vegetation model: LPJ-WHyMe v1.3.1, *Geosci Model Dev*, 3, 565-584,
9 doi:DOI 10.5194/gmd-3-565-2010, 2010.

10 Wik, M., Thornton, B. F., Bastviken, D., MacIntyre, S., Varner, R. K., and Crill, P. M.: Energy
11 input is primary controller of methane bubbling in subarctic lakes, *Geophysical Research Letters*,
12 41, 2013GL058510, doi:10.1002/2013GL058510, 2014.

13 Wolf, A., Callaghan, T., and Larson, K.: Future changes in vegetation and ecosystem function of
14 the Barents Region, *Climatic Change*, 87, 51-73, doi:10.1007/s10584-007-9342-4, 2008a.

15 Wolf, A., Kozlov, M., and Callaghan, T.: Impact of non-outbreak insect damage on vegetation in
16 northern Europe will be greater than expected during a changing climate, *Climatic Change*, 87,
17 91-106, doi:10.1007/s10584-007-9340-6, 2008b.

18 Worrall, F., Burt, T., Adamson, J., Reed, M., Warburton, J., Armstrong, A., and Evans, M.:
19 Predicting the future carbon budget of an upland peat catchment, *Climatic Change*, 85, 139-158,
20 doi:10.1007/s10584-007-9300-1, 2007.

21 Wramneby, A., Smith, B., Zaehle, S., and Sykes, M. T.: Parameter uncertainties in the modelling
22 of vegetation dynamics—Effects on tree community structure and ecosystem functioning in
23 European forest biomes, *Ecological Modelling*, 216, 277-290,
24 doi:10.1016/j.ecolmodel.2008.04.013, 2008.

25 Wrona, F. J., Prowse, T. D., Reist, J. D., Hobbie, J. E., Lévesque, L. M. J., and Vincent, W. F.:
26 Climate Change Effects on Aquatic Biota, Ecosystem Structure and Function, *AMBIO: A*
27 *Journal of the Human Environment*, 35, 359-369, doi:10.1579/0044-
28 7447(2006)35[359:CCEOAB]2.0.CO;2, 2006.

29 Yang, Z., Hanna, E., and Callaghan, T. V.: Modelling surface-air-temperature variation over
30 complex terrain around Abisko, Swedish Lapland: uncertainty of measurements and models at
31 different scales, *Geografiska Annaler: Series A, Physical Geography*, 93, 89-112,
32 doi:10.1111/j.1468-0459.2011.00005.x, 2011.

33 Yang, Z., Sykes, M., Hanna, E., and Callaghan, T.: Linking Fine-Scale Sub-Arctic Vegetation
34 Distribution in Complex Topography with Surface-Air-Temperature Modelled at 50-m
35 Resolution, *AMBIO*, 41, 292-302, doi:10.1007/s13280-012-0307-0, 2012.

36 Zhang, W., Miller, P. A., Smith, B., Wania, R., Koenigk, T., and Döscher, R.: Tundra
37 shrubification and tree-line advance amplify arctic climate warming: results from an individual-
38 based dynamic vegetation model, *Environmental Research Letters*, 8, 034023, 2013.

39

1 Table 1. Tundra heath summer and whole year NEE comparisons between the modelled and published data.

Tundra type	Arctic heath	Arctic heath	Arctic heath	Subarctic heath	LSE & HSS	LSE & HSS	LSE & HSS	LSE & HSS
Period	1997, 2000-2005, summer	2007, summer	2007, summer	2004, 13 th Jul-21 st Aug, 40 days	1961-1990, summer [§] /whole year	1991-2000, summer [§] /whole year	2001-2012, summer [§] /whole year	2051-2080, summer [§] /whole year
Location	NE Greenland	NE Greenland	NE Greenland	Northern Sweden	Northern Sweden	Northern Sweden	Northern Sweden	Northern Sweden
Methods*	EC	CH	CH	EC & CH	LPJG	LPJG	LPJG	LPJG
Cumulated	-1.4 ~ -23.3 ^a	-22.5 ^b	-18 ^b	-38.2~-68.7 ^c **	-26.89/-4.31 ^d	-41.83/-12.82 ^d	-58.23/-31.38 ^d	-67.93/-26.88 ^d

NEE

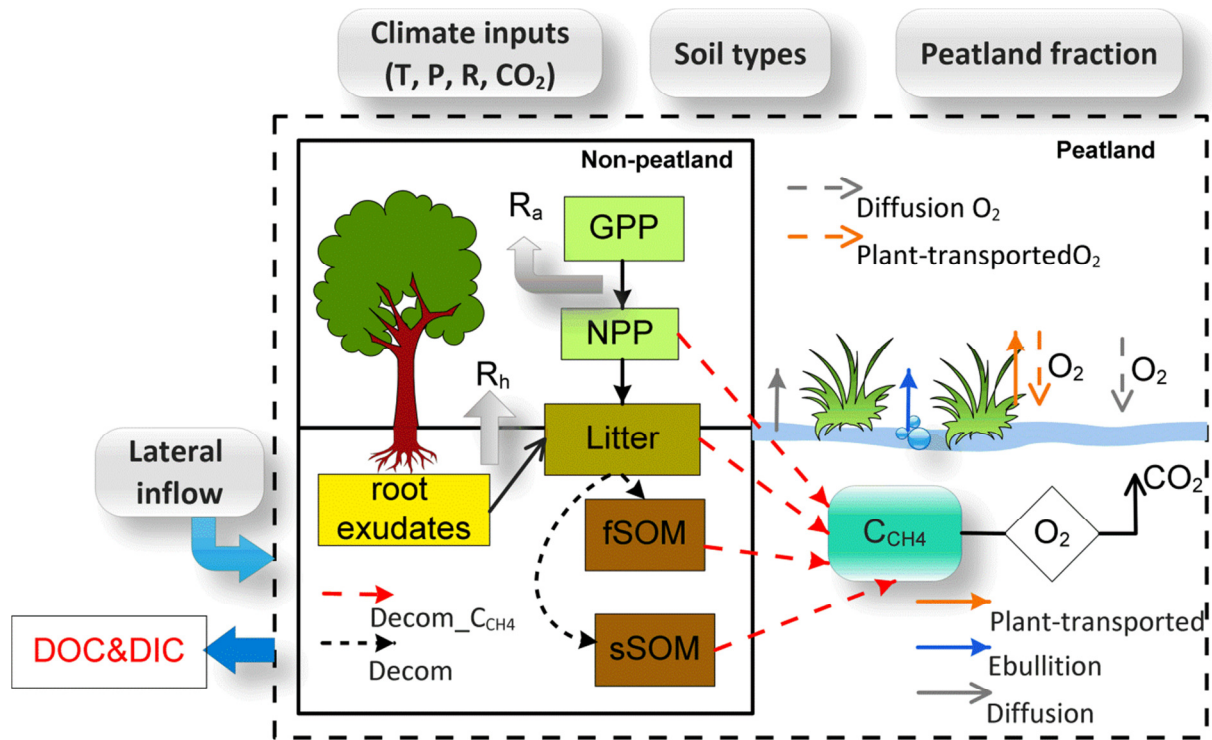
2 * EC stands for Eddy-Covariance method, CH stands for Chamber method and LPJG stands for model estimations with LPJG-WHyMe-TFM; ** values vary from
 3 sparsely vegetated areas (less than 10% cover) to fully-covered low-growing *Empetrum* areas. §: the modelled values in summer include data for June, July, August and
 4 September. LSE: low-growing (<50 cm) evergreen shrubs. HSS: tall (< 2m) deciduous shrubs. ^a:(Groendahl et al., 2007); ^b: (Tagesson et al., 2010); ^c: (Fox et al., 2008); ^d: This
 5 study.

6

1 Table 2. Summary of catchment C-budget for different time periods. Both mean and annual variations (one standard deviation value in
 2 the parentheses) of each period are presented. Negative values indicate ecosystem carbon uptake, while positive values indicate that
 3 mean ecosystem carbon is lost through respiration. The mean temperature (T, °C) of each period is listed.

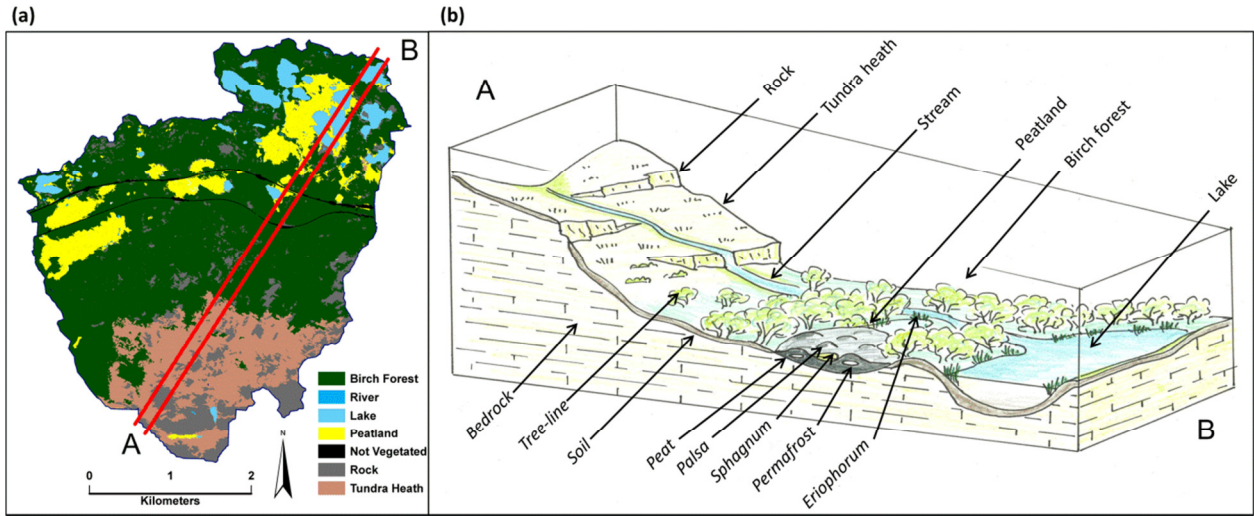
Periods	Birch CO ₂ [§]	<i>Eriop.</i> CO ₂ [§]	Palsa <i>/Sphag.</i> CO ₂ [§]	<i>Peatland</i> CH ₄	Tundra heath	Streams CO ₂ [*]	Lakes CO ₂ [*]	Streams CH ₄ [*]	Lakes CH ₄ [*]	Birch DIC	Peatlan d DIC	Birch DOC	<i>Eriop.</i> DOC	Palsa <i>/Sphag.</i> DOC	C budget
1961-1990 (T = -1.26)	-17.52 (22.46)	-36.83 (30.80)	-18.04 (31.39)	14.08 (1.57)	-4.31 (15.81)							2.52 (0.73)			-1.47 (18.25)
2000-2005 (T = 0.13)	-3.48 (34.10)	-32.85 (28.91)	-10.49 (27.36)	17.65 (2.21)	-1.63 (21.77)							3.25 (0.56)			7.96 (27.00)
2006-2011 (T = -0.19)	-56.68 (44.26)	-60.10 (25.98)	-37.26 (24.58)	18.60 (1.27)	-50.27 (27.28)							2.31 (0.67)			-38.71 (34.55)
2051-2080 (T = 0.90)	-24.56 (39.05)	-28.84 (32.25)	-8.43 (27.67)	22.94 (3.71)	-26.88 (32.22)							2.86 (0.40)			-11.23 (33.11)
Measured	0.88^a	-90.34^b	-50.18^c	20.23^{b,§}	-3^{**},^d	10.1±4.4^e	0.5±0.2^e	0.06^e	0.1±0.1^e	1.22^f	1.22^f	3.17^f	7.55^g	3.35^g	
(Years)	(2007- 2010)	(2006- 2008)	(2008- 2009)	(2006- 2007)		(2009- 2011)	(2008- 2011)	(2009- 2011)	(2010)	(2007 - 2009)	(2007- 2009)	(2008- 2009)	(2008)	(2008)	

4 [§]: fluxes taken away DOC and DIC export. [§]: observed CH₄ fluxes for the *Eriophorum* site. ^{*}: variables are normalized to the catchment area. ^{**}: is a reference-
 5 estimated value. ^a (Heliasz, 2012); ^b (Jackowicz-Korczyński et al., 2010); ^c (Olefeldt et al., 2012); ^d (Christensen et al., 2007); ^e (Lundin et al., submitted); ^f (Olefeldt et al.,
 6 2013); ^g (Olefeldt and Roulet, 2012); *Eriop.*: *Eriophorum* and *Sphag.*: *Sphagnum*.

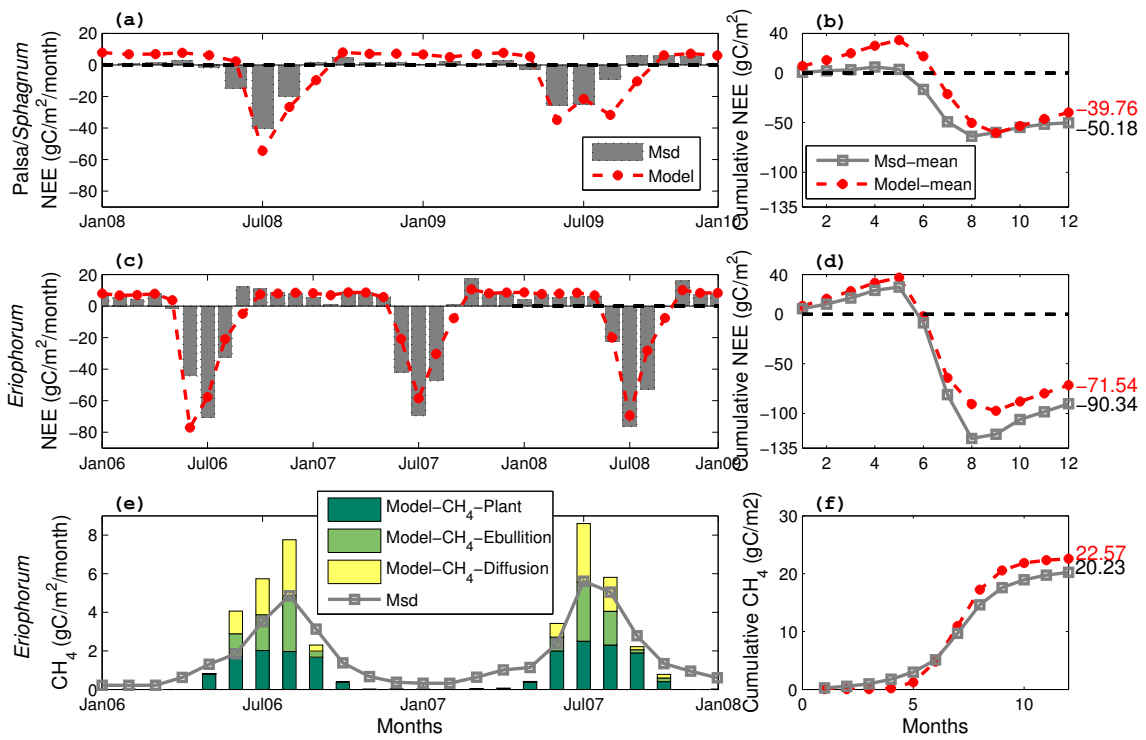


1

2 Figure 1. Schematic of carbon components and cycling in LPJG-WHyMe-TFM. The solid line-
 3 box includes carbon cycling for non-peatland cell, whereas the items inside the dashed line-box
 4 represent processes particular to the peatland cells. Only DOC&DIC in red text is not explicitly
 5 presented in the current model. T: air temperature, P: precipitation, R: radiation, CO₂:
 6 atmospheric CO₂ concentration, Decom_C_{CH4}: decomposed materials allocated to C_{CH4}, Decom:
 7 decomposition.

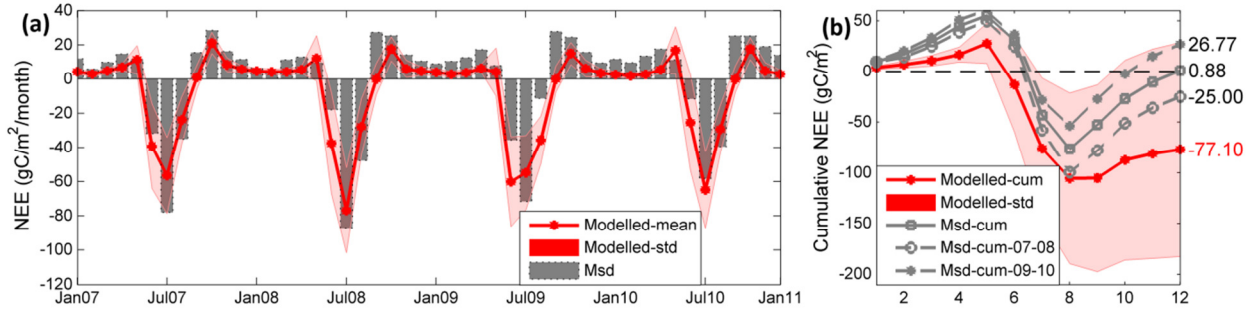


1
 2 Figure 2. Object-based vegetation classification map of the Stordalen catchment (a) and
 3 schematic of landcover types and features of the approximate transect A-B in (b).

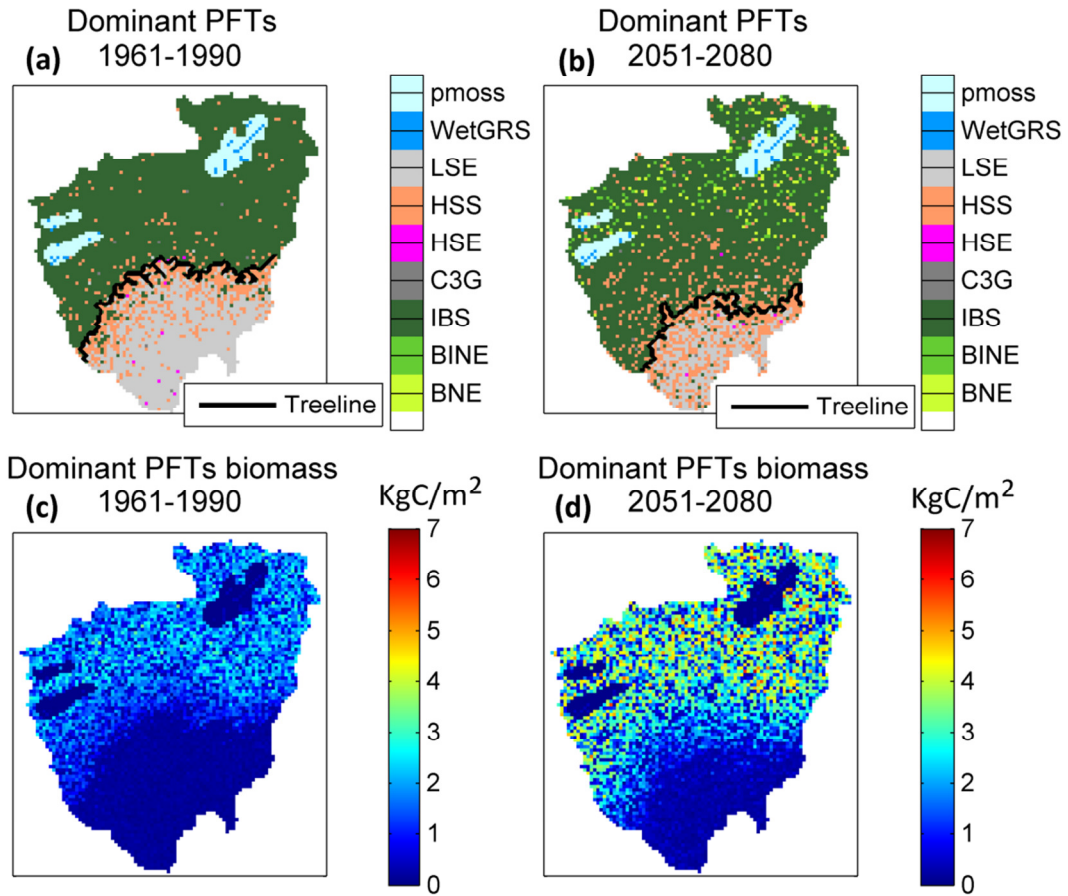


1

2 Figure 3. Monthly (left) and mean annual cumulative (right) CO₂ NEE and CH₄ fluxes for the
 3 peatland. Positive values indicate ecosystem release to the atmosphere and negative values
 4 indicate ecosystem uptake. Msd stands for Measured.

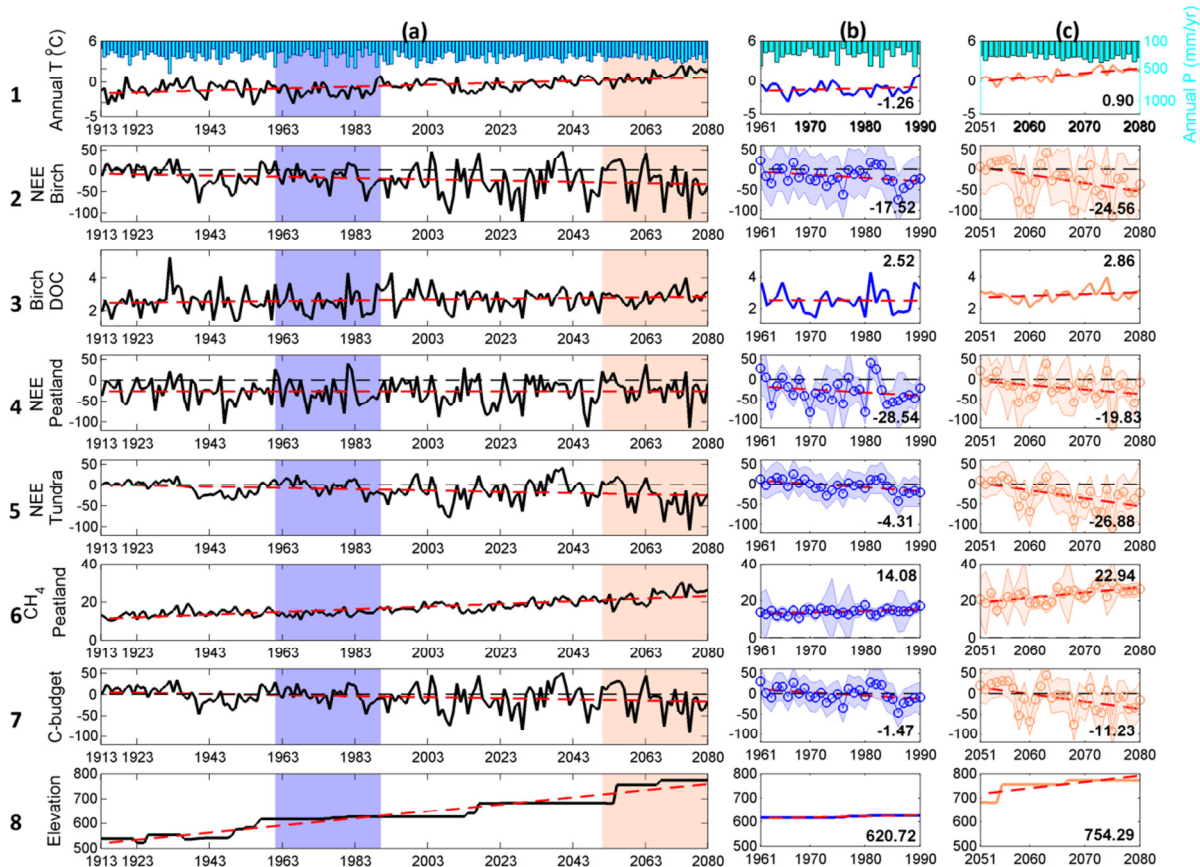


1
 2 Figure 4. Monthly (a) and cumulative (b) NEE between the years 2007 and 2010 for the birch
 3 forest. Modelled NEE with spatial variability (red shadow) for each year is shown.



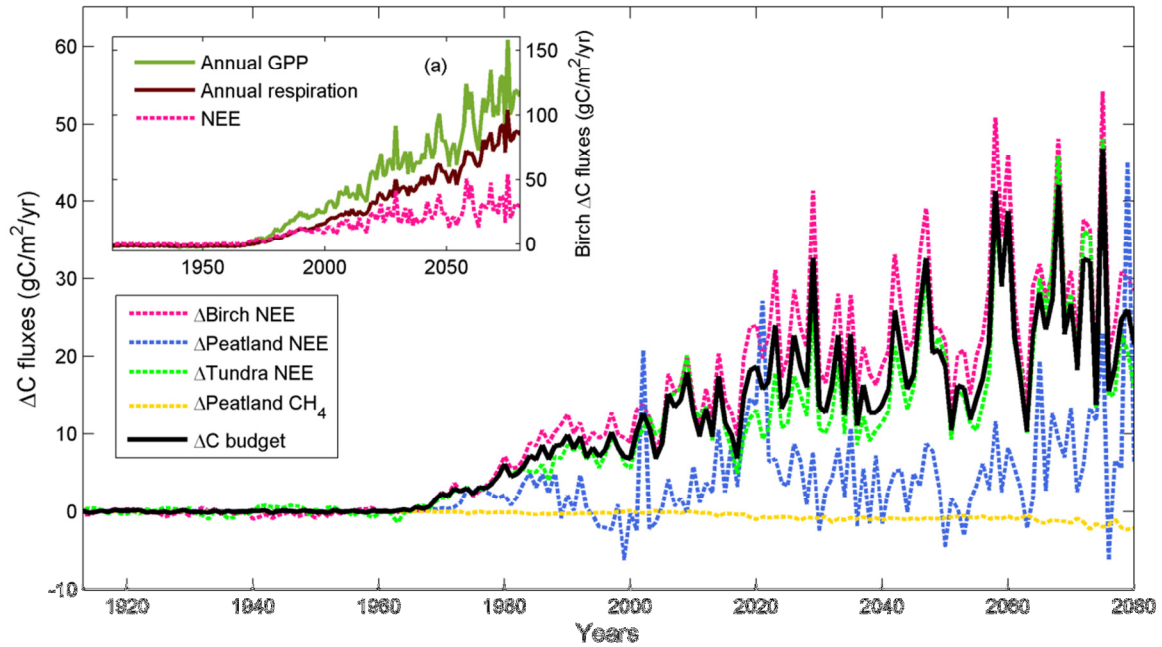
1

2 Figure 5. Dominant PFTs ((a) and (b)) and their biomass ((c) and (d)) in the study catchment, for
 3 the periods 1961-1990 ((a) and (c)) and 2051-2080 ((b) and (d)).



1
 2 Figure 6. Time-series (column a) of annual mean temperature, precipitation sum, NEE
 3 ($\text{gC/m}^2/\text{yr}$), averaged DOC export ($\text{gC/m}^2/\text{yr}$) from the birch forest, birch tree line elevation (m)
 4 and catchment C-budget ($\text{gC/m}^2/\text{yr}$) values between 1913 and 2080. The NEE data for the birch
 5 forest and the peatland have had the corresponding DOC and DIC values subtracted. Here the
 6 averaged C fluxes from the Stordalen peatland (the northeast side of the catchment) are used to
 7 represent for the averaged C fluxes for the whole catchment peatlands since only the Stordalen
 8 peatland DOC and DIC observations are currently available. The aerial photo-based
 9 classification of the *Eriophorum* and *Palsa/Sphagnum* peatland fractions within the Stordalen
 10 peatland is used to scale up the C fluxes. The trend of each dataset is shown with a red dashed
 11 line. The second and third columns (b and c) of the figure focus on the periods 1961-1990 and
 12 2051-2080 (these two periods are also indicated in the first column with shaded area). The
 13 numbers in bold type in columns b and c show the annual average of each quantity for the
 14 respective time period. The fractions of peatland, birch forest, tundra and lakes/rivers are 5.7%,

1 57.69%, 29.76% and 5%, respectively. Approximately 1.79% of the catchment area is estimated
2 as being dominated by C3G and HSE, which are not included in the above classification. The last
3 row shows the birch tree line elevation changes over the period.



1

2 Figure 7. Carbon flux differences (ΔC fluxes) for different landcover types with and without a
 3 CO_2 increase since 1960. Positive values of ΔC NEE imply a higher uptake or a lower emission
 4 of CH_4 in the simulations with a CO_2 increase compared to the simulation without a CO_2
 5 increase. For the birch forest landcover type, the differences in gross primary production (GPP)
 6 and ecosystem respiration are shown in the panel (a), where the positive values indicate a higher
 7 photosynthesis rate and a higher respiration rate in the simulations with a CO_2 increase,
 8 compared to the simulations without a CO_2 increase.